CANADIAN THESES

THÈSES CANADIENNES

NOTICE

The quality of this microfiche is heavily dependent upon the quality of the original thesis submitted for microfilming. Every effort has been made to ensure the highest quality of reproduction possible.

If pages are missing, contact the university which granted the degree.

Some pages may have indistinct print especially if the original pages were typed with a poor typewriter ribbon or if the university sent us an inferior photocopy.

Previously copyrighted materials (journal articles, published tests, etc.) are not filmed.

Reproduction in full or in part of this film is governed by the Canadian Copyright Act, R.S.C. 1970, c. C-30.

AVIS

La qualité de cette microfiche dépend grandement de la qualité de la thèse soumise au microfilmage. Nous avons tout fait pour assurer une qualité supérieure de reproduction

S'il manque des pages, veuillez communiquer avec l'université qui a conféré le grade.

La qualité d'impression de certaines pages peut laisser à désirer, surtout si les pages originales ont été dactylographiées à l'aide d'un ruban usé ou si l'université nous a fait parvenir une photocopie de qualité inférieure.

Les documents qui font déjà l'objet d'un droit d'auteur (articles de revue, examens publiés, etc.) ne sont pas microfilmés.

La reproduction, même partielle, de ce microfilm est soumise à la Loi canadienne sur le droit d'auteur, SRC 1970, c. C-30.

THIS DISSERTATION HAS BEEN MICROFILMED EXACTLY AS RECEIVED

LA THÈSE A ÉTÉ MICROFILMÉE TELLE QUE NOUS L'AVONS REÇUE

Canada

Analytical and Experimental Study on the Behaviour of Prestressed and Poststressed Composite Girders

Abdolrahim Nouraeyan

A Thesis

in

The Department

of

Civil Engineering

Presented in Partial Fulfillment of the Requirements
for the degree of Master of Engineering at
Concordia University
Montréal, Québec, Canada
June 1987

ISBN 0-315-37093-9

ABSTRACT

Analytical and Experimental Study on the Behaviour of Prestressed and Poststressed Composite Girders.

Abdolrahim Nouraeyan

Tests and theoretical investigation on the behaviour of Prestressed and Poststressed Composite Girders are presented in this thesis. The type of beam used in this study was of W-rolled steel beam with concrete slab of 2 inch thick on its top flange. Prestressing and Poststressing was applied by means of high strength steel tendons with different configuration along the span.

Two quarter-scale models were tested as a simply supported beams. A total of four sets of tests were conducted on these two models. Additional tests were also carried out on steel, cable and concrete specimens to verify the mechanical properties of the materials used in this study.

An analytical methode was selected and improved for predicting the stresses developed along the span, increments in initial tendon force and deflection of these girders. The analysis was based on an assumed perfect shear connection between concrete slab and steel girder. In addition ,the effects of losses caused by creep, shrinkage and tendon relaxation together with residual stresses in steel beam were neglected. Calculated results were then compared, an attempt was also made to find differences in behaviour between prestressing and poststressing composite girders.

ACKNOWLEDGEMENT

The author wishes to express his gratitude to Drs. M. S. Troitsky and Z.A. Zielinski for their invaluable advice and guidance throughout the research program and during the preparation of this thesis.The financial assistance provided from research grants is appreciated.

The author wishes to thank Dr. K. Ghavami for his valuable comments. Thanks are also due to Messrs. D. Roy and R. Lombardo for their assistance during the experimental phase of the research program. The assistance of Mr. Pichett of BBR company for supplying the prestressing equipment is gratefully acknowledged.

Finally, the author wishes to thank his family for their endless love, support and understanding at all times, and also wishes to thank his friends for their assistance. Thanks are also due to Miss Cathy Duff for typing this thesis.

TABLE OF CONTENTS

LIST OF FIGURES

LIST OF TABLES

NOTATIONS

A_c	-	Concrete cross section area
A_{cp}	-	Transfer composite cross section area
A_s	-	Steel cross section area
A_{cb}	-	Tendon cross section area
E_c	-	Modulus of elasticity of concrete
E_{cb}	-	Modulus of elasticity of steel cable
E_s	-	Modulus of elasticity of steel beam
e_{cp}	-	Eccentricity of tendon with respect to neutral axis of compsoite section
e_s	-	Eccentricity of tendon with respect to neutral axis of steel section
I_c	-	Moment of inertia of concrete section
I_{cp}	-	Moment of inertia of transformed composite section
I_s	-	Moment of inertia of steel section
K	-	Distance between wheel load in MS-250-77 truck loading
L	-	Span of the girder
L_t	-	Length of prestressing/poststressing tendon
M^{DL}	-	Dead load moment
M^{SD}	-	Superimposed dead load moment
M^{LL+I}	-	Live load and impact load moment
N-A	-	Neutral axis of section
P	-	Prestressing/poststressing force
q	-	Uniformly distributed load

S_g^t	-	Section modulus of steel section with respect to top fiber of steel
S_g^b	-	Section modulus of steel section with respect to bottom fiber of steel
S_{cp}^t	-	Section modulus of composite section with respect to top fiber of concrete
$S_{cp}^{t.s}$	-	Section modulus of composite with respect to top fiber of steel
S_{cp}^b	-	Section modulus of composite section with respect to bottom fiber of steel
T	-	Single shaft truck loading influence by impact effect
$\Sigma\sigma_c^t$	-	Sum of stresses at top fiber of concrete
$\Sigma\sigma_g^t$	-	Sum of stresses at top fiber of steel
$\Sigma\sigma_g^b$	-	Sum of stresses at bottom fiber of steel
$2\Delta P^{DC}$	-	Force increase in tendon due to concrete weight
ΔP^{SD}	-	Force increase in tendon due to superimposed dead load
ΔP^{LL+I}	-	Force increase in tnedon due to live load and impact
$\delta^{PR/PO}$	-	Upward deflection due to prestressing/poststressig force at mid span
δ_B^T	-	Deflection under point load "B" due to truck loading
δ^{UDL}	-	Deflection due to uniformly distributed load

CHAPTER 1

INTRODUCTION

1.1 OBJECTIVES

Although the concept of prestressing and poststressing of composite girder by means of high strength tendon is not new, common practice shows that this particular method of construction is not widely used as compared to the conventional composite girder. The reason why this particular construction technique has not been widely used is due to the lack of engineering information on the overall behaviour of prestressed and poststressed composite girders. A study is required to elaborate the overall behaviour of prestressed and poststressed composite girders with different tendon configurations in terms of stresses along the span, increment of prestressing and poststressing forces, and upward deflections. As shown in Fig. 1.1, prestressing and poststressing of a simply supported beam can be achieved by means of high strength tendons with different configurations.

The objective of this research study is to find the most suitable, desirable and economical tendon configuration. Furthermore, an additional investigation is needed to find the differences in behaviours between prestressed and poststressed composite girders. The outline of research works established for this study includes:

1. To review the available literature for information regarding prestressed and poststressed composite girders.
2. To select and improve an analytical method for the elastic behaviour of prestressed and poststressed composite girders.

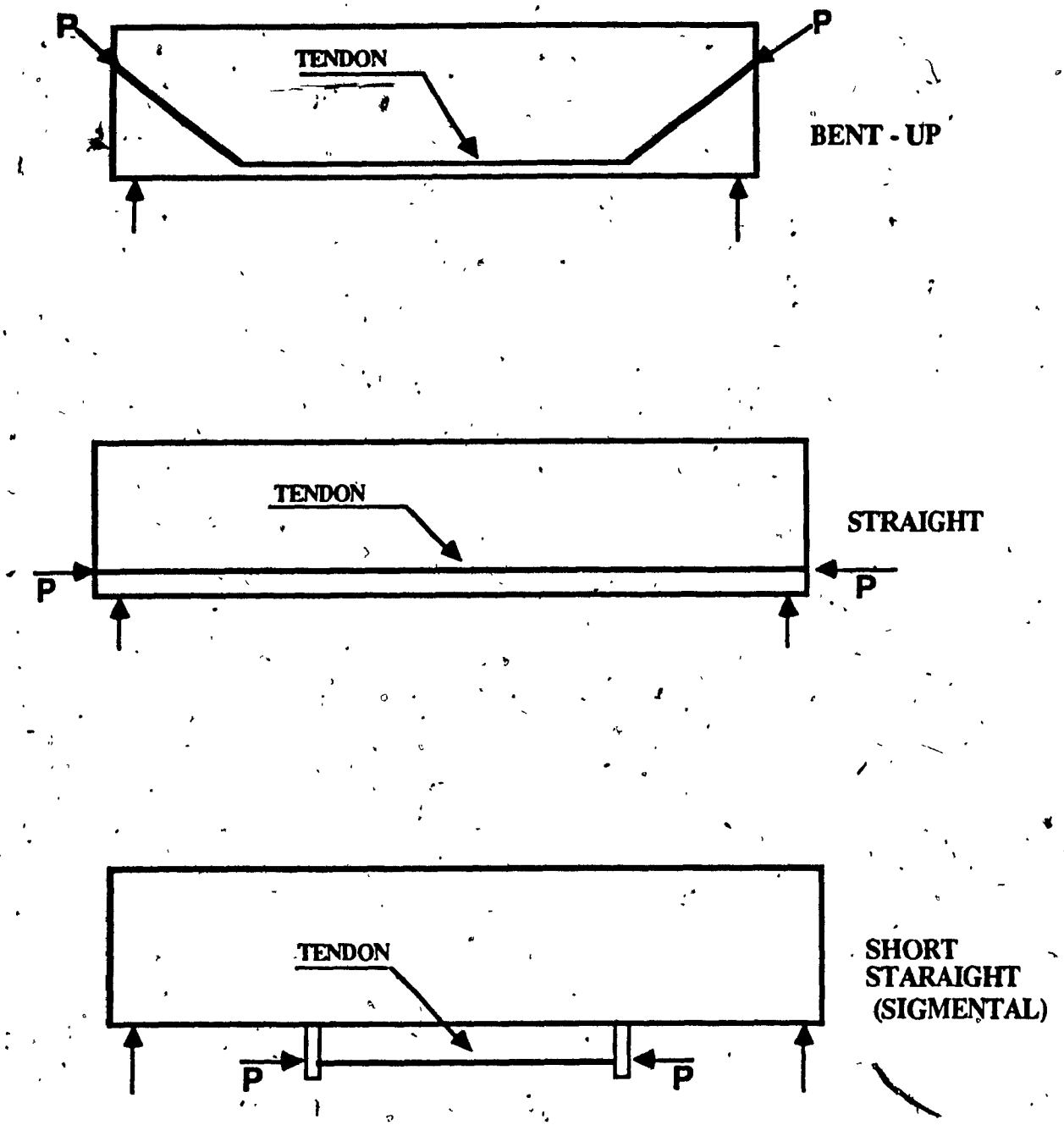

FIG 1.1:- DIFERENT TENDON CONFIGURATIONS

3. Verify the analytical method by comparing it with a quarter-scale model girders constructed in the Concordia University Structure Laboratory.

1.2 LITERATURE REVIEW

The literature review which follows has been organized into two main topics; prestressed composite girders and poststressed composite girders.

In 1959 R. Szilard [8] published a paper dealing with the design of postressed composite structures using a parabolic tendon configuration along the span. The analysis was based on the assumption of a perfect shear connection between the concrete slab and the steel beam. In his analysis, the "increased modular ratio method" was used to determine the final stresses under permanent loads.

Tachibana et al [9] studied experimentally the behaviour of two composite beams with bent-up tendons. They concentrated mainly on the strain variation in concrete slab in transverse direction at mid span of the beam under poststressing force. In their conclusion, it was ntoed that a prestressed composite beam has a nearly equal bearing capacity as the poststressed composite beam even though they showed different crack loads.

In 1967 an incremental strain method of analysis was proposed by R.S. Reagan [6]. In his analysis he assumed that the strain distribution across the cross section of the concrete slab and steel beam to be linear, except for a discontinuous jump at the junction of the concrete slab and steel beam as shown in Fig. (1.2). The analysis was based on a straight tendon configuration. After analysing a series of bridge and building beams Reagan concluded that failure generally occured by crushing the concrete rather than by fracture of the tendon. Reagan also noted that unbonded tendon do not significantly affect the resistance of the beam to the deflection since the poststressing tendon does not effect the moment of inertia of the beam.

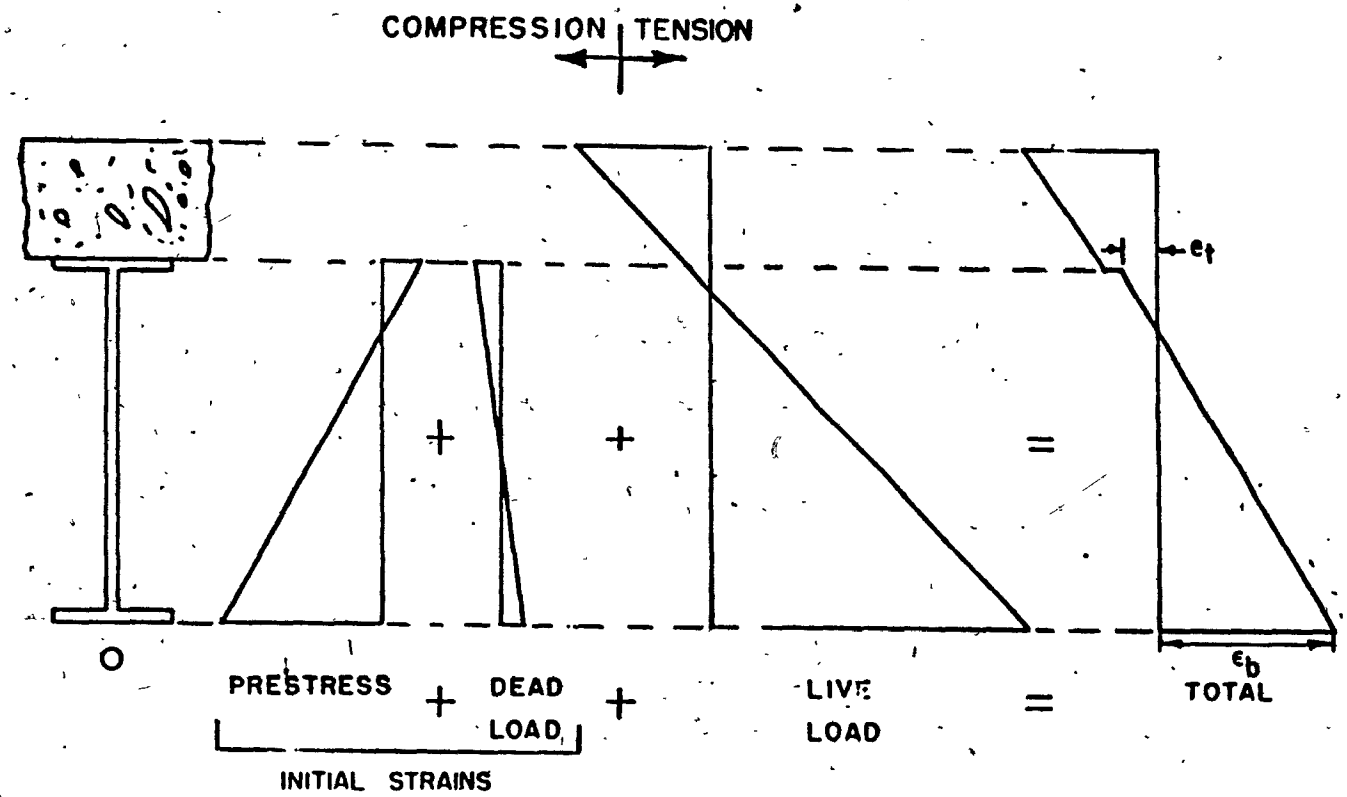

Fig. 1.2 Strain Distribution at a Typical Beam Cross Section

Stras [7] tested three poststressed composite beams, beams A, B, and C all of which had the configuration shown in Fig. 1.3. He used the "transformed section" theory to predict the behaviour of the test beams in the elastic range of stresses for the steel beam and cable.

In 1963, Hoadly [3] published a paper in which he discussed the behaviour of simply supported composite beams prestressed by means of high strength straight cables along the span. In his analysis the prestressed steel beam carries the dead weight of the structure (prestressed). He also compared the behaviour of prestressed composite beams with that of the same beam which had not been prestressed and shows a significant increase in load carrying ability obtained by prestressing.

Abbott [1] studied the effects of prestressing steel beams with horizontal restrained tendons both theoretically and experimentally. In his study he used the elastic beam theory to calculate the resulting stresses along the span, the upward deflections and buckling of the bottom flange under the effect of prestressing force. He concluded that the theoretical stress and deflection equations based on beam theory gave results comparable to the experimental values and that the bottom flange need to be stiffened with restraining diaphragm to insure that the tendon assumed the same deflected shape as the beam.

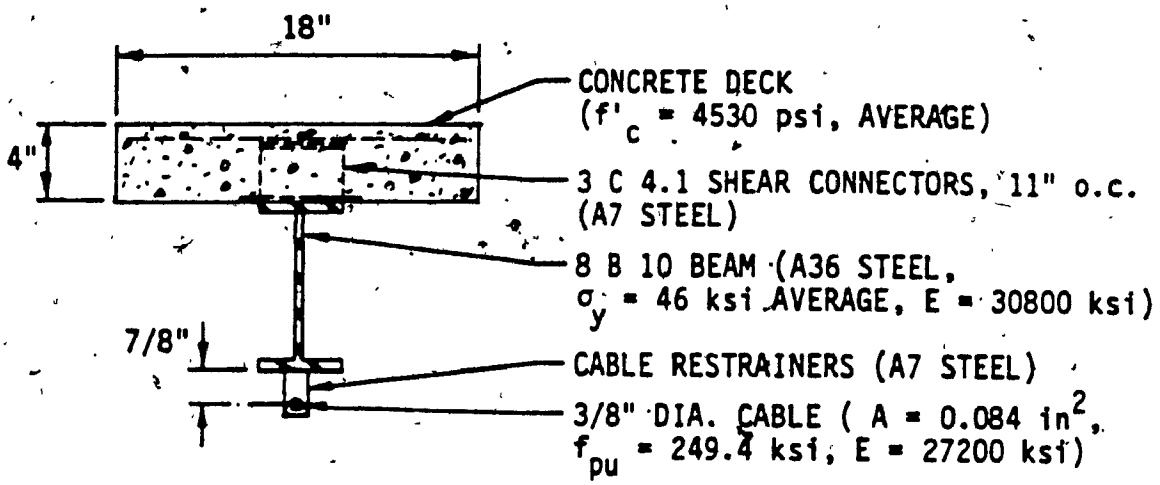

a. Cross section for Beams A, B, and C

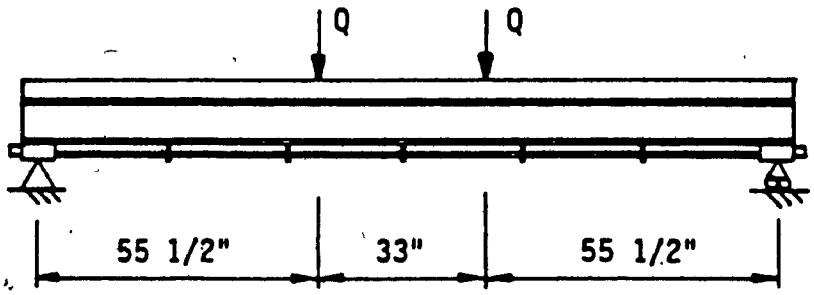

b. Elevation

Fig. 1.3 Prestressed Composite Beams [7]

CHAPTER 2

THEORETICAL ANALYSIS

2.1-INTRODUCTION :

A simply supported prestressed and poststressed composite steel and concrete beam is analysed. The concrete slab was cast on the top flange of the steel beam, meaning that the steel section alone carrying the total dead weight. The prestressing and poststressing tendons were unattached along the span, anchored at their ends and supported at saddles in case of bent up tendon configuration.

The analysis performed below is based on the following assumptions.

1 - A perfect shear connection exist between the concrete slab and the steel girder,(i . e no slip or uplift).

2 - Losses caused by creep, shrinkage and tendon relaxation were neglected.

3 - Residual stresses in the steel beam were neglected.

The composite section have been transformed into an equivalent steel section using the ratio of modulus of elasticity of the two materials.

$$n = E_s/E_c \qquad (2.1)$$

Where:

E_s=Modulus of elasticity of steel .

E_c=Modulus of elasticity of concrete .

2.2 LOADING SYSTEMS :

The analysis is done for the case of simply supported bridge girder. In the design and analysis of prestressed and poststressed composite girder of simple span bridges, two type of loading are considered.

A) - The uniformly distributed loading along span such as a dead load of steel, concrete and superimposed load which produces a bending moment as shown in the Fig2.1.

Reactions under uniform loading is given by:

$$R_{1D} = R_{2D} = q\ L/2 \qquad (2.2)$$

The bending moment due to uniformly distributed loading at mid span is:

$$M_D = M_{max} = q\ L^2/8 \qquad (2.3)$$

The magnitude of bending moment due to uniformly distributed in point "B" is:

$$M_D = M_B = q\ (0.125\ L^2 - 0.0137K^2) \qquad (2.4)$$

B) - In case of simple span bridge of up to 150 ft the governing loading in design (based on Canadian Code for Highway Bridge Design CAN3-S6-M78) is a truck loading as shown in Fig 2.

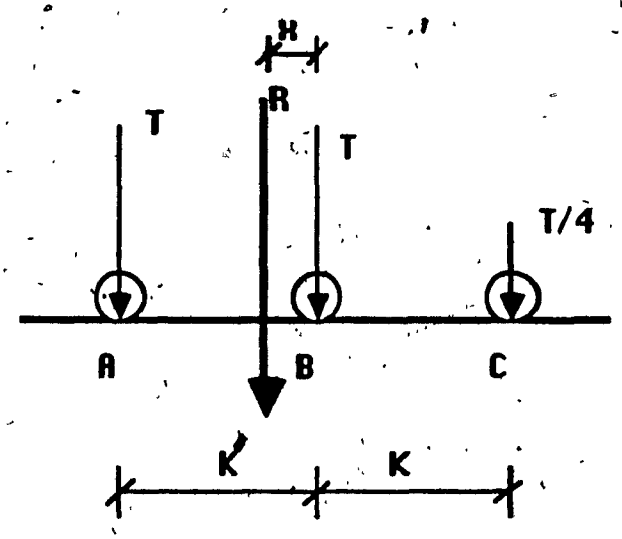

FIG 2 :- MS-TRUCK LOADING

AB = Variable spacing of 14 feet to 28 feet

BC = Constant spacing of 14 feet

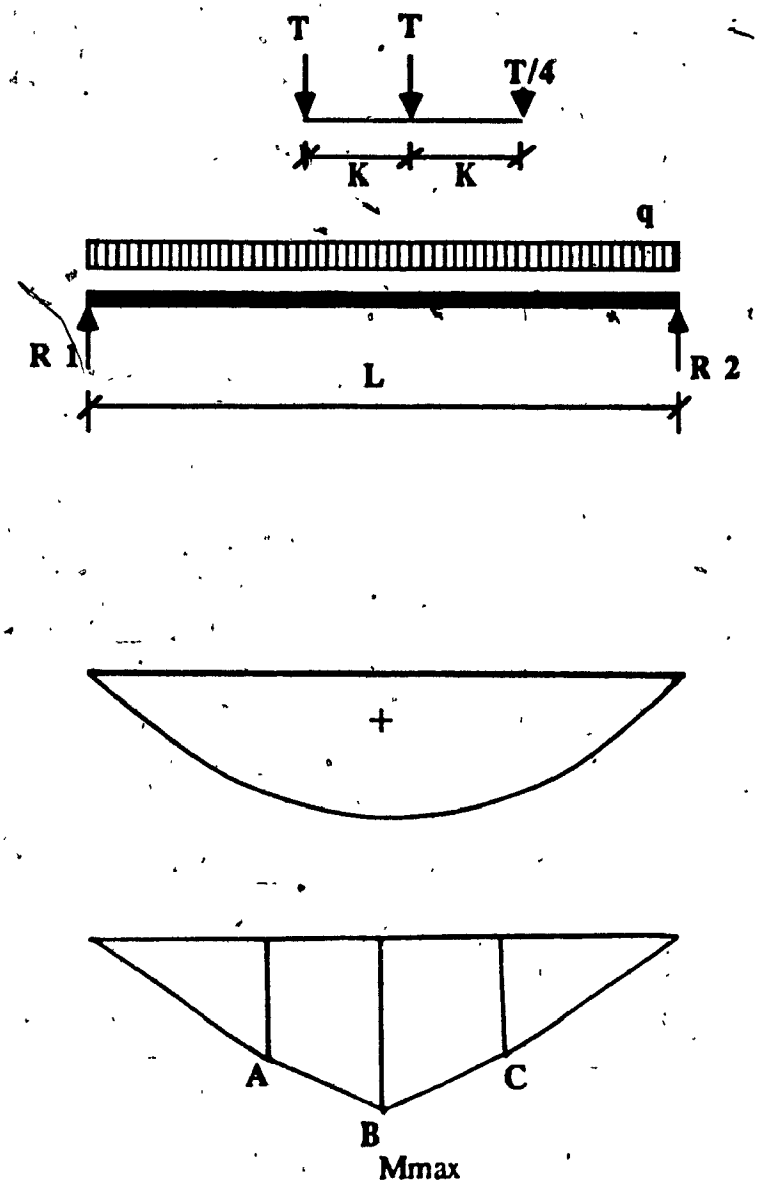

FIG 2.1:- BENDING MOMENT DIAGRAM FOR TRUCK LOADING AND UNIFORMLY DISTRIBUTED LOADING.

Table 2.1 shows type of truck loading used in the design of the highway bridges in Canada. In this loading system the ratio of 1:1:1/4 exist between the wheels A,B and C.

LOADING #	A=T	B=T	C=T/4
MS250-77	200kN	200kN	50kN

Table 2.1 MS 250 - 77 LOADING

By influence line diagram as well as code recommendation the maximum bending moment will be obtained when distance AB=BC=K=4.25 m (14-ft), and occurs under the wheel load "B" when the resultant (R) of the truck loading(A, B & C) and wheel load "B" are in equal distance (0.166K) from the mid span of the girders as shown in Fig 2.1.

Reactions under truck loading, are given by Equations (2.5&2.6).

$$R_{1t} = T(1.125 + 0.376\ K/L) \qquad (2.5)$$

$$R_{2t} = T(1.00 + 0.376\ K/L) \qquad (2.6)$$

Maximum bending moment due to truck loading under point load B can be evaluated by Equation(2.7).

$$M_{Bt} = M_{max} = T(0.5625L - 0.625K + 0.062K^2/L) \qquad (2.7)$$

Maximum bending moment due to truck loading at mid span can be evaluated by equation (2.8).

$$M_{mid} = T\,(\,0.5625\,L - 0.8334\,K - 0.062K^2/L) \qquad (2.8)$$

Total bending moment at mid span due to uniform dead and truck load:

$M_{M.S}$ = Equations (2.3 + 2.8)

Total bending moment under point load B due to dead and live load:

M_B = Equations (2.4 + 2.7)

The maximum of the above equations give the critical moment.

2.3-BENT-UP TENDON :

The bent up tendon produces a moment along span as shown in Fig 2.2. The magnitude of this moment along the span is given by equations (2.9) and(2.10).

Between saddles and supports M=Pex/a (2.9)

Between the two saddles M=P(e) (2.10)

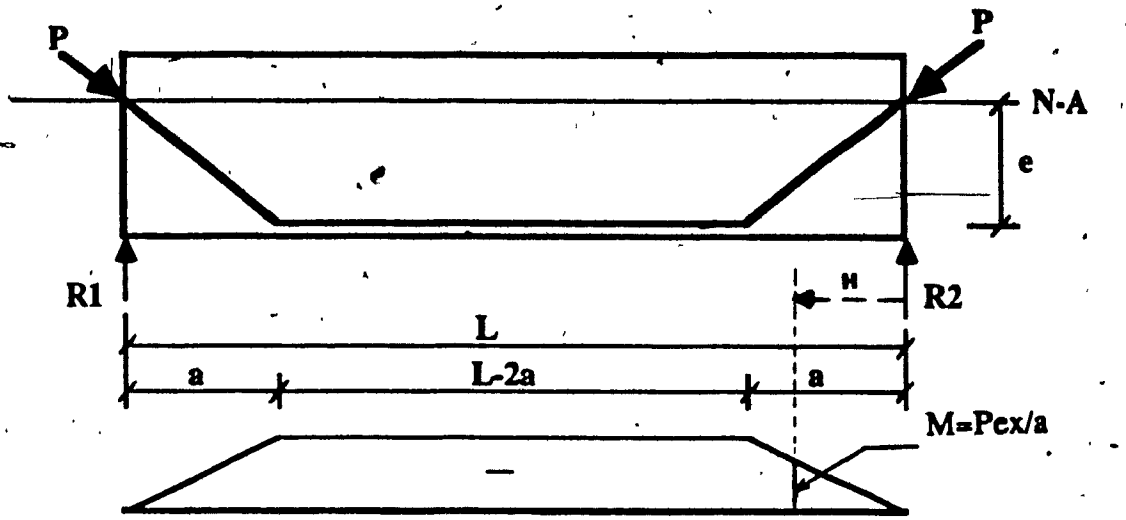

FIG 2.2 :-BENDING MOMENT DIAGRAM DUE TO TENDON FORCE

Under the application of the external load, there will be a certain increment in the initial tendon force.

This increment can be found using virtual work method [2]. Assuming that the cable and beam are cut in the middle, and displacements of the cable and beam under external load and cable actions are compared.

$$\delta_{1P} + \Delta P\, \delta_{11} = 0 \qquad (2.11)$$

Where

δ_{ip} = Displacement due to tendon force

ΔP = Increment due to applications of external load

δ_{11} = Displacement due to unit load

then, increment is:

$$\Delta P = -\frac{\delta_{1P}}{\delta_{11}} \qquad (2.12)$$

From Equation (2.12) the following expression have been developed.

a) Increment due to truck loading is given by Equation (2.11),(Ref. to Fig 2.1):

$$\Delta P = \frac{Te\left[0.2812\,L^2 - 0.5314\,K^2 - 0.5\,a^2\right]}{L\left\{\frac{e_{cp}^2(3L-4a)}{3} + \frac{L\,I_{cp}}{A_{cp}} + \frac{E_s I_{cp}}{E_{cb} A_{cb}}\left[L + \frac{2a}{\cos^3\alpha}(1-\cos^3\alpha)\right]\right\}} \qquad (2.13)$$

b) Increment due to uniformly distributed loading is given by Equation 2.12 (Ref. to Fig 2.1)

$$\Delta P = \frac{-qe\left[L^3 - a^2(2L-a)\right]}{12L\left\{\frac{e_{cp}^2(3L+4a)}{3} + \frac{L\,I_{cp}}{A_{cp}} + \frac{E_s I_{cp}}{E_{cb} A_{cb}}\left[L + \frac{2\,a}{\cos^3\alpha}(1-\cos^3\alpha)\right]\right\}} \qquad (2.14)$$

2.4 - STRAIGHT TENDON :

In this case cables are placed at a constant eccentricity from the neutral axis along the span, as shown in Fig 2.3.

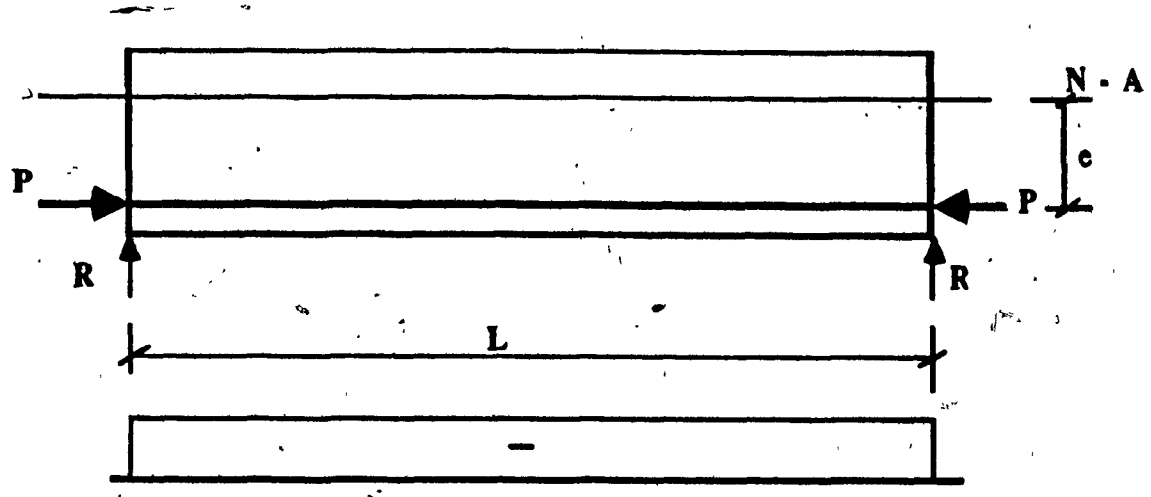

FIG 2.3:- BENDING MOMENT DIAGRAM DUE TO TENDON FORCE

The magnitude of moment is given by:

$$M = P\,e \qquad (2.15)$$

The increment in initial prestressing force can be find in similar way as in the case of bent up tendon (section 2.3) which resulted in the following equations.(2.16 & 2.17)

a) Increment due to truck loading is: (Ref. to Fig 2.1).

$$\Delta P = \frac{Te\ (0.2812\,L^2 - 0.5314\,K^2)}{L\left[e_{\varphi}^2 + \frac{I_{\varphi}}{A_{\varphi}} + \frac{E_s I_{\varphi}}{A_{\phi} E_{\phi}}\right]} \qquad (2.16)$$

b) Increment due to uniformly distributed load is: (Ref. to Fig 2.1).

$$\Delta P = \frac{qL\,e_{cp}}{12\left[e_{cp}^2 + \frac{I_{cp}}{A_{cp}} + \frac{E_s I_{cp}}{A_b E_b}\right]} \qquad (2.17)$$

2.5 - SHORT STRAIGHT TENDON (Lt < L):

In this case, a straight tendon of constant eccentricity is provided shorter than the span as shown in the Fig 2.4 .

The magnitude of the moment produced will be :

$$M = P\,e \qquad (2.18)$$

The increment can be found by the similar method (section 2.3 , 2.4).

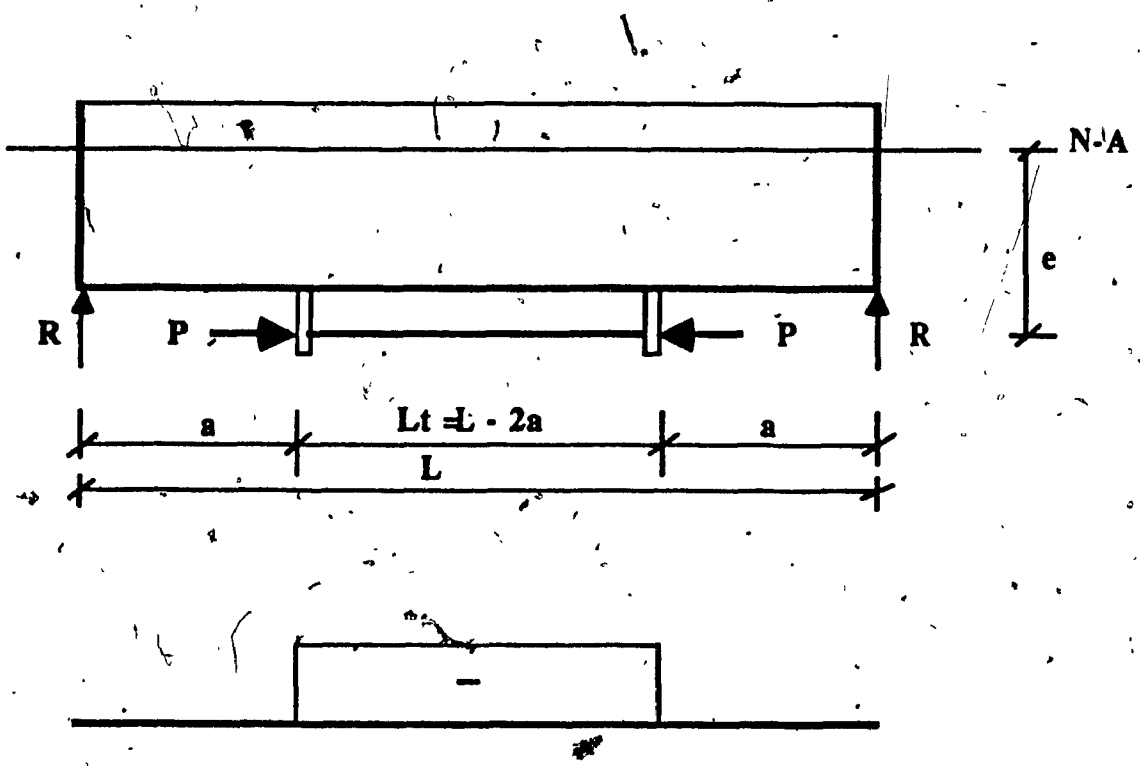

FIG 2.4:- BENDING MOMENT DIAGRAM DUE TO TENDON FORCE

a) Increment due to truck loading is given by Equation (2.19).(Ref. to Fig 2.1).

$$\Delta P = \frac{Te_{cp}\left[0.2812\,L^2 - 0.5314\,K^2 - 1.5a^2\right]}{(L-2a)\left[e_{cp}^2 + \frac{I_{cp}}{A_{cp}} + \frac{EI_{cp}}{A_{cb}E_{cb}}\right]} \qquad (2.19)$$

b) Increment due to uniformly distributed loading is given by Equation (2.20). (Ref. to Fig 2.1).

$$\Delta P = \frac{qe_{cp}\left[a(L-a) + \frac{L^2}{2}\right]}{6(L-2a)\left[e_{cp}^2 + \frac{I_{cp}}{A_{cp}} + \frac{EI_{cp}}{A_{cb}E_{cb}}\right]} \qquad (2.20)$$

2.6 - STRESS ANALYSIS :

The stresses imposed on the member due to prestressing/poststressing are of opposite direction to those imposed by the service load, that is the cable force normally causes small tensile stresses in the top fiber and large compressive stresses in the bottom fibers of simply supported beams. While the superimposed dead load and live load which are to be carried by the beam cause tensile stress in the bottom fibers and compressive stresses in the top fiber.

Based on the assumption made at section (2.1). The following equations were derived to obtain the stresses at specific (critical) section of the girder . They are the modified form of the basic equations of stresses .

NOTE: In the following stress equations the (-) sign stay for the compression component and (+) sign for tension component.

A)- PRESTRESSED COMPOSITE GIRDER :

In this type of structure the loading sequence is as follows:-

1) Steel weight.
2) Prestressing.
3) Concrete weight. — On steel section only.
4) Increment due to concrete weight.

5) Superimposed dead load.
6) Increment due to superimposed dead load. — On composite section.
7) Live load influances by impact.
8) Increment due to live load & impact....

Under the above loading sequence the stresses developed at different fibers considering different sections can be evaluated by the following equations.Equation (2.21) gives the final stresses at top fiber concrete.

Fig (2.5) shows the stress diagram under each stage of loading.

$$\sum \sigma_c^t = \frac{1}{n}\left[- \frac{M^{SD} + M^{LL+I}}{S_{cp}^t} \right] \qquad (2.21)$$

Equation (2.22) gives the final stresses at top fiber steel.

$$\sum \sigma_s^t = - \frac{M^{DL}}{S_s^t} - \frac{M^{SD} + M^{LL+I}}{S_{cp}^{ts}} + (\Delta P^{SD} + \Delta P^{LL+I})\left(\frac{e_{cp}}{S_{cp}^{ts}} - \frac{1}{A_{cp}}\right) +$$

$$+ P\left(\frac{e_s}{S_s^{ts}} - \frac{1}{A_s}\right) + \Delta P^c \left(\frac{e_s}{S_s^{ts}} - \frac{1}{A_s}\right) \qquad (2.22)$$

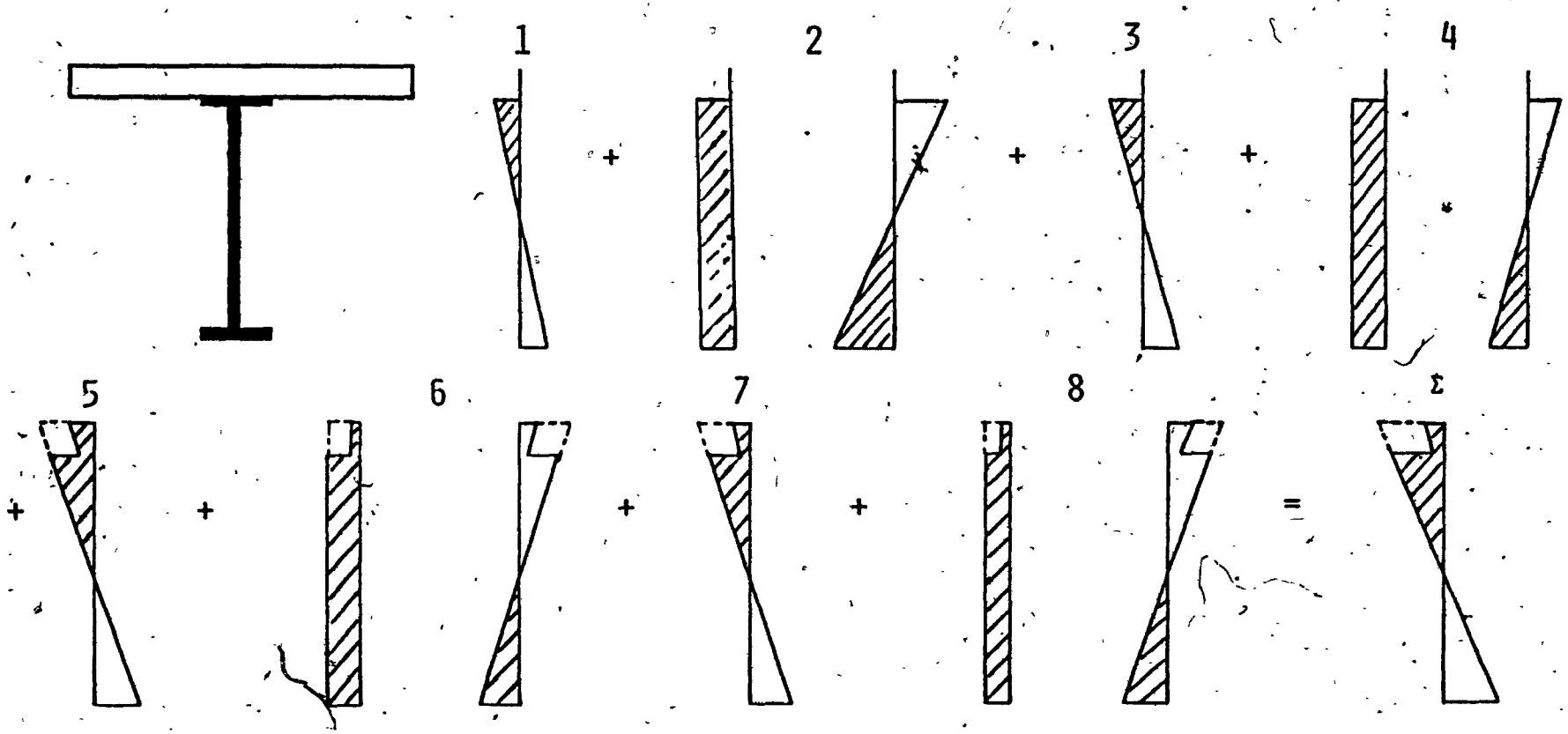

FIG. 2.5:- STRESS DIAGRAM FOR PRESTRESSED COMPOSITE GIRDER AT MID SPAN UNDER EACH STAGE OF LOADING

COMPRESSION

TENSION

Equation (2.23) gives the final stresses at bottom fiber steel.

$$\sum \sigma_s^b = \frac{M^{DL}}{S_s^b} + \frac{M^{SD} + M^{LL}}{S_{cp}^b} - (\Delta P^{SD} + \Delta P^{LL+I})\left(\frac{e_{cp}}{S_{cp}^b} + \frac{1}{A_{cp}}\right) -$$

$$- P\left(\frac{e_s}{S_s^b} + \frac{1}{A_s}\right) - \Delta P^c \left(\frac{e_s}{S_s^b} + \frac{1}{A_s}\right) \qquad (2.23)$$

B)- POSTSTRESSED COMPOSITE GIRDER:-

In this type of structure the loading sequence is as follows

---

1) Steel weight.
2) concrete weight. On steel section only.

---

3) Poststressing.
4) Superimposed dead load.
5) Increment due to superimposed dead load. On composite section.
6) live load + impact.
7) Increment due to live load &impact.

Under the above loading sequence the stresses developed at different fibers considering different sections can be evaluated by the following equations.

Equation (2.24) gives the final stresses at top fiber concrete.

$$\sum \sigma_c^t = \frac{1}{n}\left[- \frac{M^{SD} + M^{LL+I}}{S_{cp}^t} + (P + \Delta P^{SD} + \Delta P^{LL+I})\left(\frac{e_{cp}}{S_{cp}^t} - \frac{1}{A_{cp}}\right)\right] \qquad (2.24)$$

Equation (2.25) gives the final stresses at top fiber steel.

$$\sum \sigma_s^t = -\frac{M^{DL}}{S_s^t} - \frac{M^{SD}+M^{LL+I}}{S_{cp}^{Ls}} + (\Delta P^{SD} + \Delta P^{LL+I})\left(\frac{e_{cp}}{S_{cp}^{Ls}} - \frac{1}{A_{cp}}\right) +$$

$$+ P\left(\frac{e_{cp}}{S_{cp}^{Ls}} - \frac{1}{A_{cp}}\right) \qquad (2.25)$$

Equation (2.26) gives the final stresses at bottom fiber steel.

$$\sum \sigma_s^b = \frac{M^{DL}}{S_s^b} + \frac{M^{SD}+M^{LL+I}}{S_{cp}^b} - (\Delta P^{SD} + \Delta P^{LL+I})\left(\frac{e_{cp}}{S_{cp}^b} + \frac{1}{A_{cp}}\right) -$$

$$- P\left(\frac{e_{cp}}{S_{cp}^b} + \frac{1}{A_{cp}}\right) \qquad (2.26)$$

Under the above loading sequence Fig (2.6) shows the stresses diagrams under each stage of loading .

2.7 - ECCENTRICITY EFFECT

In most of the existing composite girder the concrete slab have been design to carry certain amount of compression, so it is not desirable to produce any tension in the concrete slab due to poststressing force. Equation (2.27) gives the stresses developed at top fiber of the concrete slab due to poststressing.

$$\sigma_t^c = \frac{1}{n}\left[-\frac{p}{A_{cp}} + \frac{p \cdot e_{cp}}{S_{cp}^t}\right] \qquad (2.27)$$

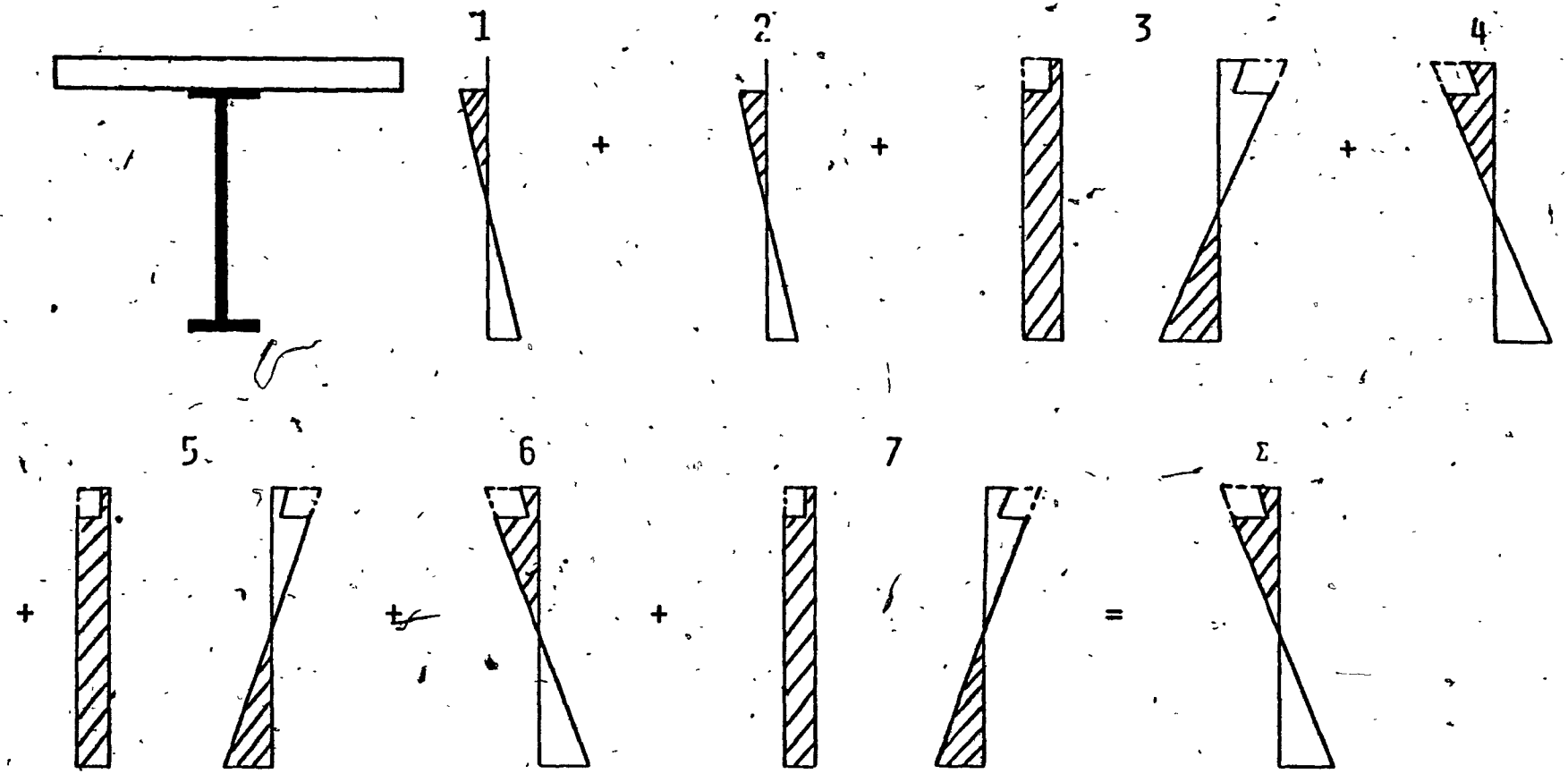

FIG. 2.6:- STRESS DIAGRAM FOR POSTSTRESSED COMPOSITE GIRDER AT MID SPAN UNDER EACH STAGE OF LOADING

COMPRESSION

TENSION

By equating Equation (2.27) to zero (assuming no tension at top fiber of concrete); a new Equation (2.28) will be developed which is independent of the amount of poststressing force and gives the maximum possible eccentricity for poststressing tendon from the neutral axis of the composite section.

$$e_{max} = \frac{S^t_{cp}}{A_{cp}} \qquad (2.28)$$

By providing poststressing tendon within this distance (e_{max}) there will be no tensile stresses in the concrete slab and the stress diagram due to poststressing force will be as shown in Fig (2.7)

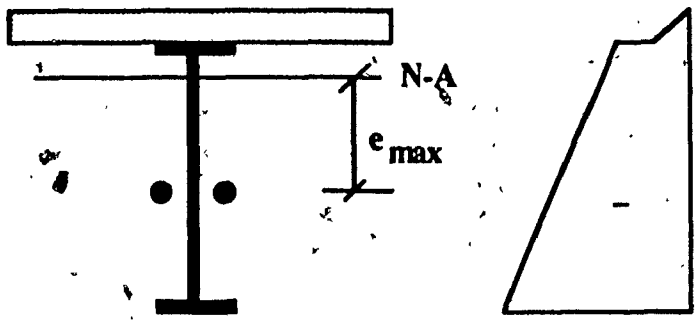

FIG. 2.7 - STRESS DIAGRAM: DUE TO POSTSTRESSING FORCE WHEN THE TENDONS ARE PLACED WITHIN THE e_{max} DISTANCE

In this case the following points are of interest.

1- At bottom fiber of steel, the full advantage of getting compression stress due to poststressing is reduced. It means that more poststressing force is required to obtain the desired stress.

2- If the tendons are far from the bottom flange, the poststressing force will be transferred to

the beam through the web, meaning that a special end block has to be designed.

3- The compression stress at top fiber of steel will increase.

2.8 - DEFLECTION.

The following equations were used to calculate the deflection.

a) Deflection under uniformly distributed load.

Maximum deflection at mid span of the beam under uniform load is:

$$\delta^{UDL} = \frac{5\,q\,L^4}{384\,EI} \qquad (2.29)$$

b) Deflection due to truck loading at point load "B".

With reference to section 2.2 and Fig 2 and 2.1, the max deflection under truck loading can be calculated using Equation (2.30).

$$\delta_B^T = \frac{T}{3EIL}(A + B + C) \qquad (2.30)$$

where

$$A = \frac{1}{4}(0.25L^4 + 0.6327\,K^4 - 3.4205\,K^2L^2 - 0.1666\,KL^3 - 0.7051\,K^3L)$$

$$B = (0.25\,L^2 - 0.0275\,K^2)^2$$

$$C = \frac{1}{16}(0.25\,L^4 + 0.2798\,K^4 - 1.555\,K^2L^2 + 0.336\,K^2L)$$

c) Upward deflection due to prestressing/poststerssing force at mid span.

Following are the equations used to find the deflection for each of the tendon configurations.

Bent-up tendon:

Referring to Fig(2.2), deflection can be calculated using Equation (2.31).

$$\delta^{PR/PO} = -\frac{(P + \Delta P)e}{24EI}(3L^2 - 4a^2) \qquad (2.31)$$

Straight tendon:

Referring to Fig(2,3), deflection can be calculated using Equation (2.32).

$$\delta^{PR/PO} = -\frac{(P + \Delta P)\, eL^2}{8EI} \qquad (2.32)$$

Short-straight tendon:

Referring to Fig(2.4), deflection can be calculated using Equation (2.33).

$$\delta^{PR/PO} = \frac{-(P + \Delta P)e}{8EI}(L^2 - 4a^2) \qquad (2.33)$$

The change in deflection due to applied loads and prestressing/poststressing force for each of the cable configuration are shown in Chapter 4 .

The experimental deflection were measured by means of mechanical dial gauges as discussed at section (3.6.B). The accuracy of the measurment was 0,001 IN.

CHAPTER 3

EXPERIMENTAL PROGRAM

3.1-INTRODUCTION:

The experiment program consist of testing two prestressed and poststressed composite girders with different tendon configurations and loaded with similitude of real loading. From these tests, which represents some particular combinations of parameters, the following questions could then be answered.

1 - Can the stresses at top fiber of concrete; top and bottom fibers of steel caused by the cable force be predicted by the common equation ($-P/A \pm Pe/S$ equations 2.21 - 2.26) ?

2 -Do the deflections of the girder during construction and under service load agree with equations 2.30 through 2.33 ?

3 -Can the increase in the initial tension of the tendon (ΔP) be predicted by equations 2.13, 2.14, 2.16, 2.17, 2.19 & 2.20 ?

3.2 - DIMENSIONS OF THE MODELS:

Two rolled (W310X24) steel sections each of 19' 7" long were used.The concrete slab is 18 inch wide and 2 inch thick for both prestressed and postsdtressed composite section.

3.3-SIMILITUDE CONDITION :

In this study the materials used for the model construction were the same as those of the prototype design. With respect to geometry, Table(3.1) shows the similitude ratio between the prototype and model.

Comparing rows 3 &4 of Table 3.1, it can be seen that the differences in their values are less then 8%, therefore these models can be considered as a satisfactory models and no correction factor is required for the results obtained during the tests.

The superimposed uniform load was applied through lowering of suspended balast (connected to the crane in the structures laboratory) as shown in Fig. 3.1. The magnitude of this loading was 121 lb per ft of span.

TABLE 3.1 :-Geometrical comparison ratio between the prototype and the model .

	Depth In.	Flange Thickness In.	Flange Width In.	Web In.	C/S Area Sq-Ins.	Wt lb/ft	Moment of inertia $In.^4$	Span In.
PROTOTYPE	48	1	16	1	78	265.2	25786	912
MODEL	12	0.26	4	0.23	4.71	16	103	228
MODEL SIMILARITY RATIO	4	3.84	4	4.34	16.56	16.57	250.34	4
SIMILARITY RATIO FOR TRUE MODEL	4	4	4	4	16	16	256	4

Similutude truck loading were applied through the hydraulic jacks mounted on the testing frame as shown in Fig. 3.2.

The supports used in these models were made in such a way as to simulate the effects of a real bridge. These supports were knife edge at one end and a rolling system at the other, as shown in Fig 3.3.

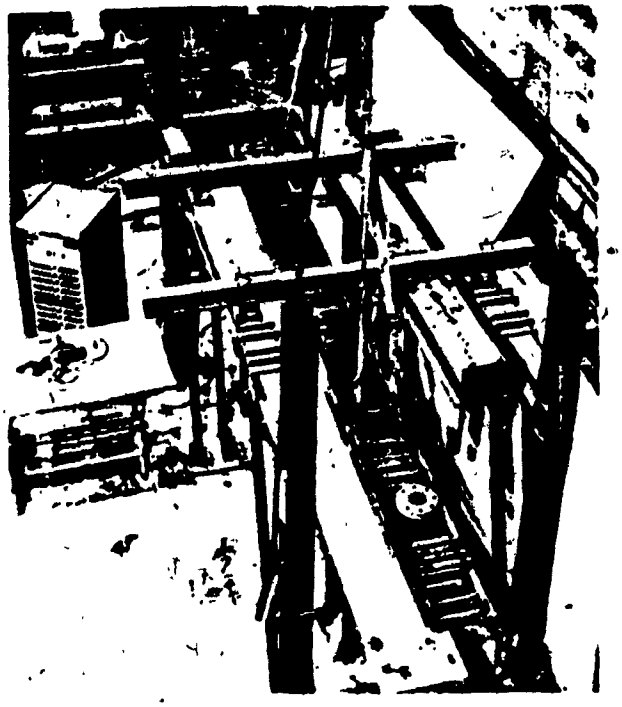

FIG. 3.1 :- View of the arrangement for the superimposed dead load application.

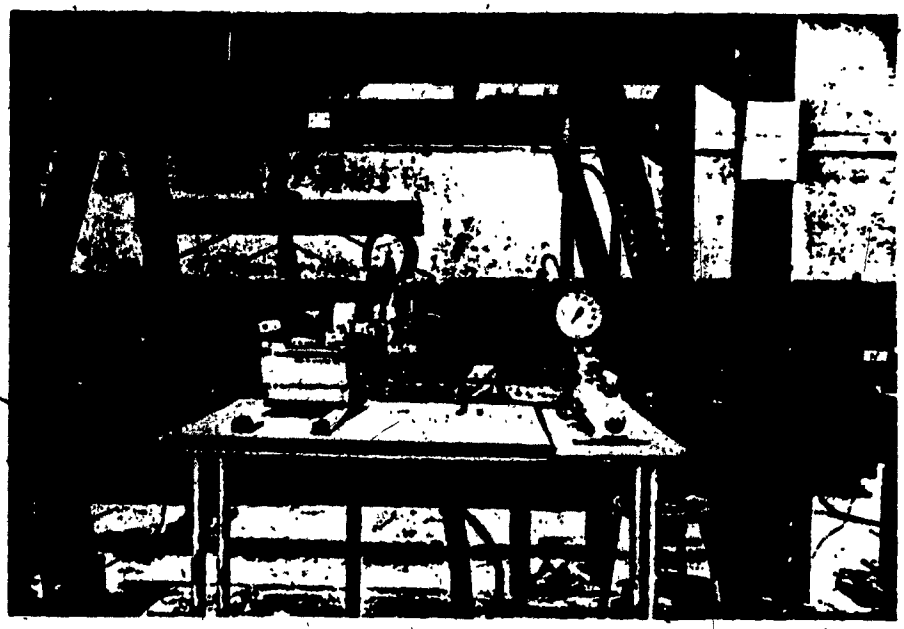

FIG. 3.2- View of the arrangement for the similtude truck loading.

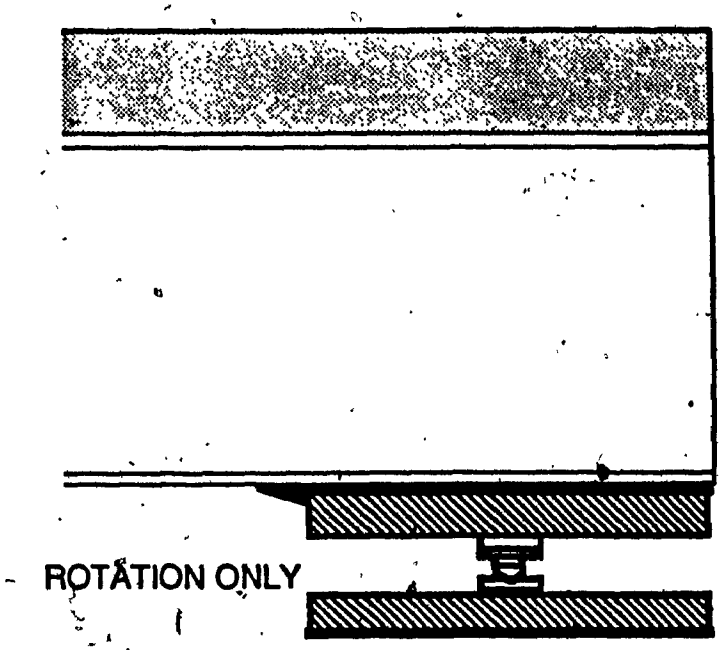

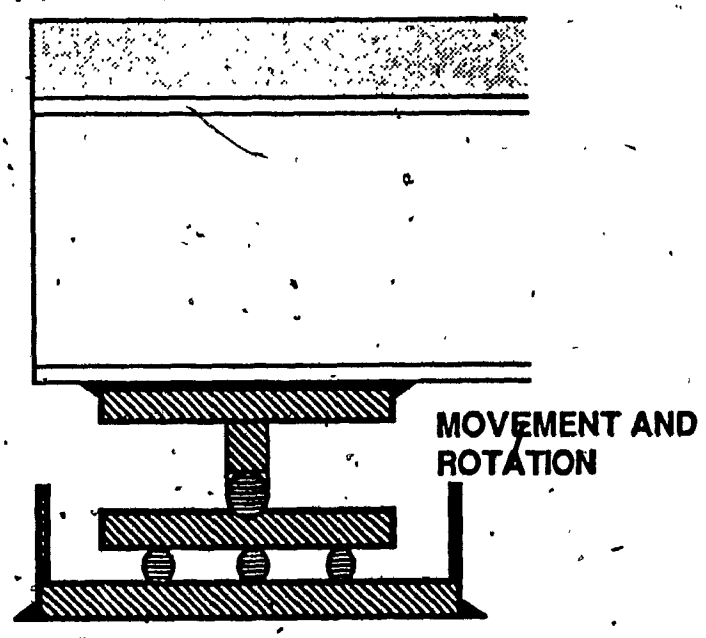

FIG 3.3:- Bearing system used in these experiments.

3.4 - MATERIALS :

3.4.1 - STEEL BEAMS:

The steel rolled beams were **W310X24** were used. Both beams were cut from the same piece to ensure uniformity. Table (3.2) shows the properties and dimensions of the rolled beam used. The properties are shown in Table 3.2 which were verified through measurements and tests.

Table 3.2: Properties and dimension of the steel beam.

DESIGNATION:-	W310X24
NOMINAL MASS:-	16 LB/FT
TOTAL CROSS SECTION AREA:-	4.71 IN^2
MOMENT OF INERTIA:-	103 IN^4
SECTION MODULUS :-	17.2 IN^3
DEPTH:-	11.99 IN
FLANGE WIDTH:-	3.99 IN
FLANGE THICKNESS:-	0.26 IN
WEB THICKNESS:-	0.23 IN
YIELD STRESS:-	44 KSI
MODULUS OF ELASTICITY:-	29000 KSI

3.4.2 - STEEL CABLES:

The prestressing/poststressing cables used were 7-wire strands of nominal diameters, 3/8" and 5/8". Table 3.3 shows the properties of these strands.

TABLE 3.3: -Important properties of the strands used

NOMINAL DIAMETER In..	AREA, SQ.In..	WEIGHT lb/ft	f_{pu} KSI	0.7 f_{pu} Aps KIP
3/8 In.	0.080	0.27	250	14.0
5/8 In.	0.215	0.74	250	37.6

3.4.3 - CONCRETE:

MODEL "A" - The concrete used was mixed manualy in the structures laboratory in one batch and for half cubic meter of concrete the following proportion was used.

CEMENT- 2.5 sacks type I portland cement.

SAND- 500 pound.

GRAVEL- 750 pound ≤1/2 Inch .

WATER- 3.5 gallons.

Table 3.4 shows the compression strength tests for the concrete cylinders at different ages.

TABLE 3.4 :- Compression test results on the concrete specimens.(Model A)

AGE IN DAYS	f'c - PSI	REMARKS
7	2495	W_c = 140 lb/ft^3 (normal weight)
14	2980	f'c = 3979 PSI
21	3592	(Empirical formula given by ACI - 8.5.1) $E_c = 57000\sqrt{f'c}$
28	3979	$E_c = 3.564 \times 10^6$ PSI

MODEL "B"

For this model, ready mixed fast cured concrete was used Table 3.5 shows the compression strength test for the concrete cylinder at different ages. Shown strength are average values for three to five sample tests.

Table 3.5 - Compression test results on the concrete specimens (Model B)

AGE IN DAYS	f'c - PSI	REMARKS
7	2366	W_c = 140 lb/ft^3 (normal weight)
14	2891	f'c = 3870 PSI
21	3522	
28	3870	E_c = 3.564 x 10^6 PSI

3.4.4 -SHEAR CONNECTORS

Steel bolts of 0.5 In. diameter and 1.5 In. long were used as shear connectors. Two steel bolts were welded on the top flange at 8 In. spacing longitudinally as shown in Fig. 3.4.

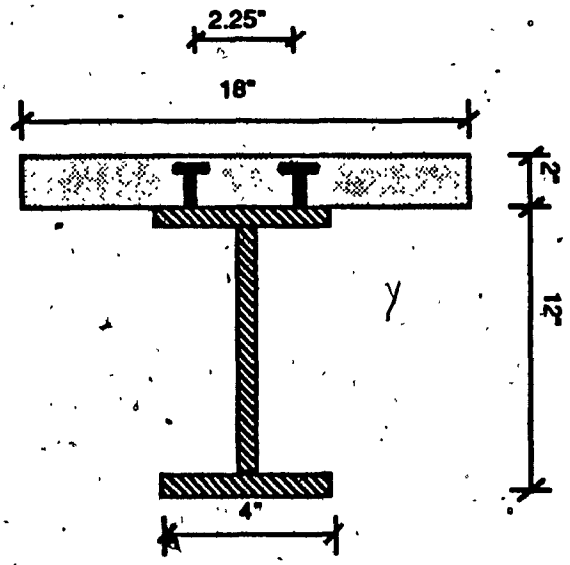

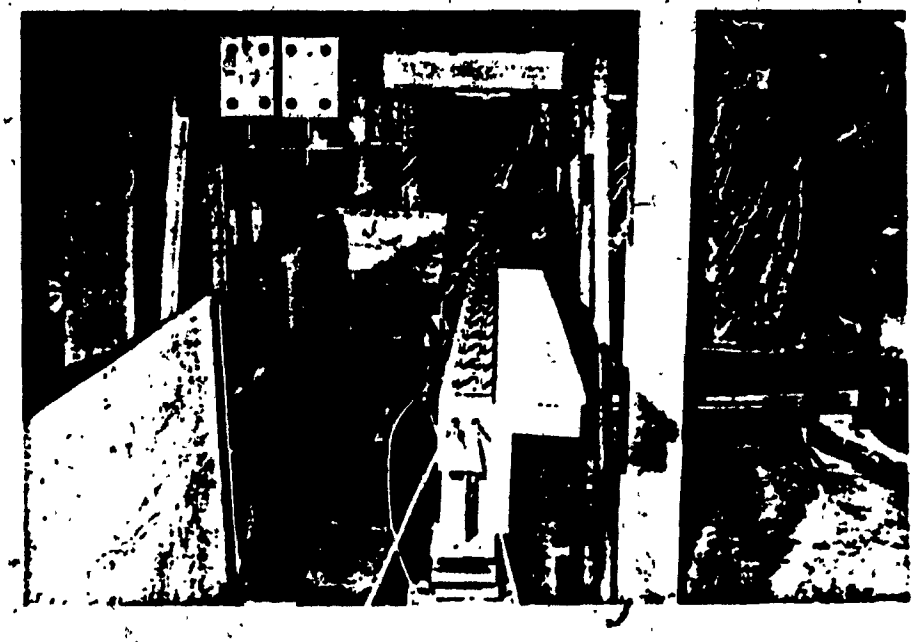

FIG. 3.4 :-Shear connectors arrangement along the span.

3.4.5-ANCHOR BLOCKS AND CHOCKS

Two sizes of friction anchor chocks were used for two different cable sizes as shown in Fig. 3.5. To distribute the concentrated tendon force, steel angles were welded to the flange, web,or both at the tendon ends as shown in Fig. 3.7 to 3.9. The tendon force was transfered to these angles through a 1inch thick steel plate.

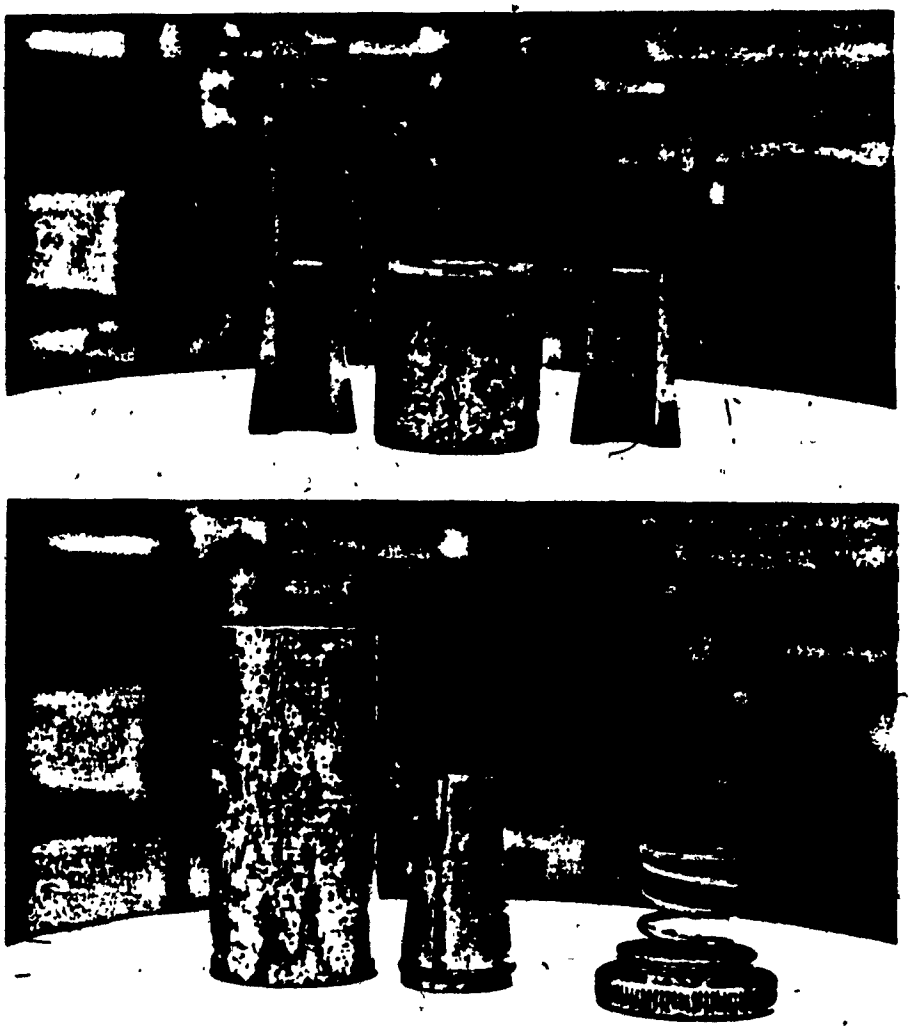

FIG. 3.5 :-Anchor chock arrangements used in these experiments.

A) BENT UP TENDON:-

To hold the cables at the desired eccentricity along the span , a pulley system was used as shown in Fig. 3.6.

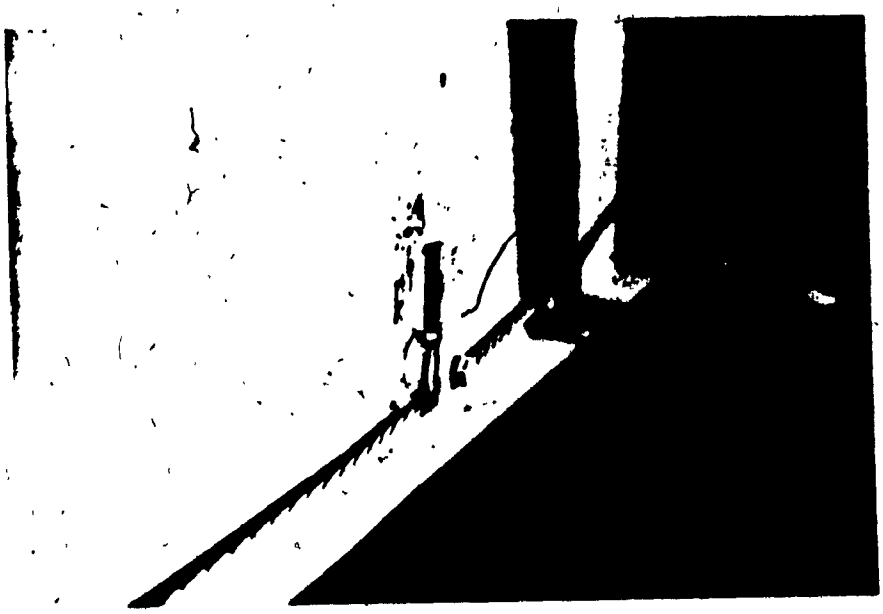

FIG. 3.6 :-Pulley system used in bentup tendon configurations.

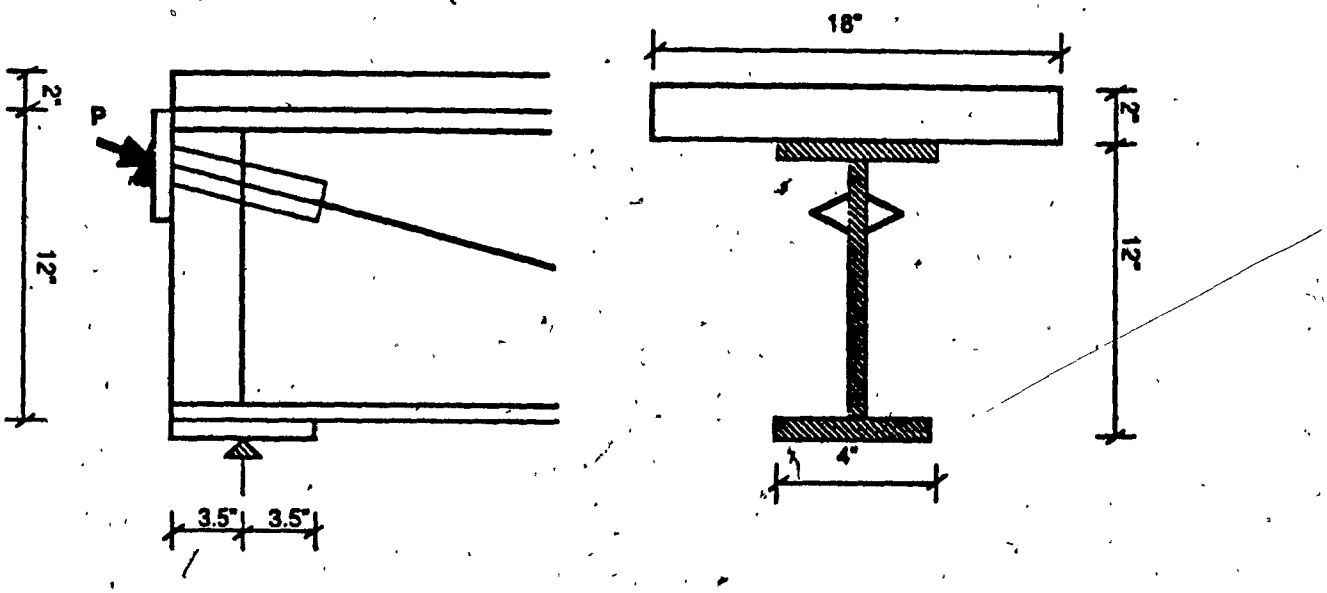

FIG. 3.7 :- Cable configuration and end block arrangement for bentup tendon.

B) STRAIGHT TENDON:-

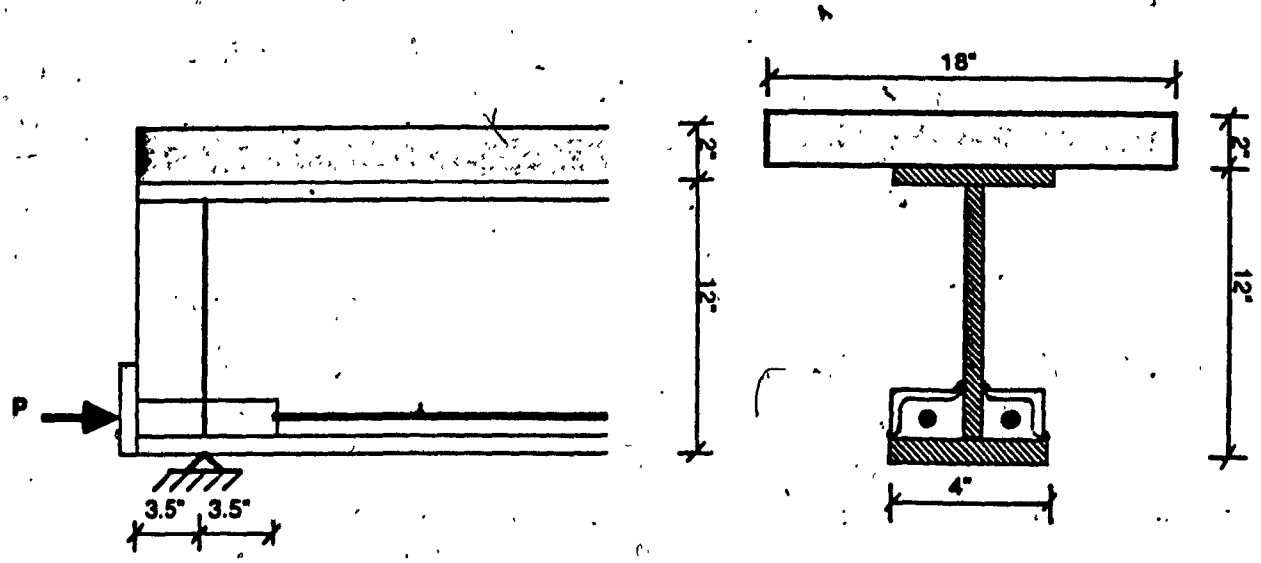

FIG 3.8 :- Cable configuration and end block arrangement for straight tendon.

C) SHORT STRAIGHT TENDON ($L_t < L$):-

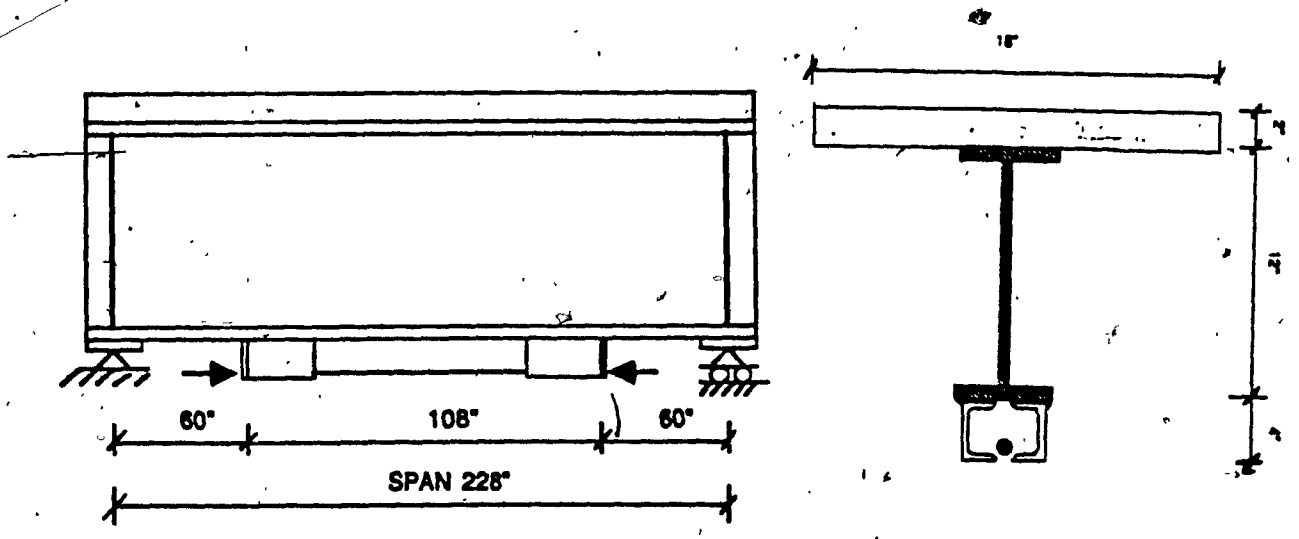

FIG 3.9 :- Cable configuration and end block arrangement for short straight tendon.

3.5 : TESTING FRAME:

The girder specimen was placed under a testing frame for loading purposes. Fig. 3.10 shows the testing frame with a girder prepared for loading. Each girder was simply supported with a span of 19-ft . The three concentrated loads which represent the similitude truck loading, adjusted for impact effect, were applied by means of jacks mounted to the testing frame(see Fig 3.2).

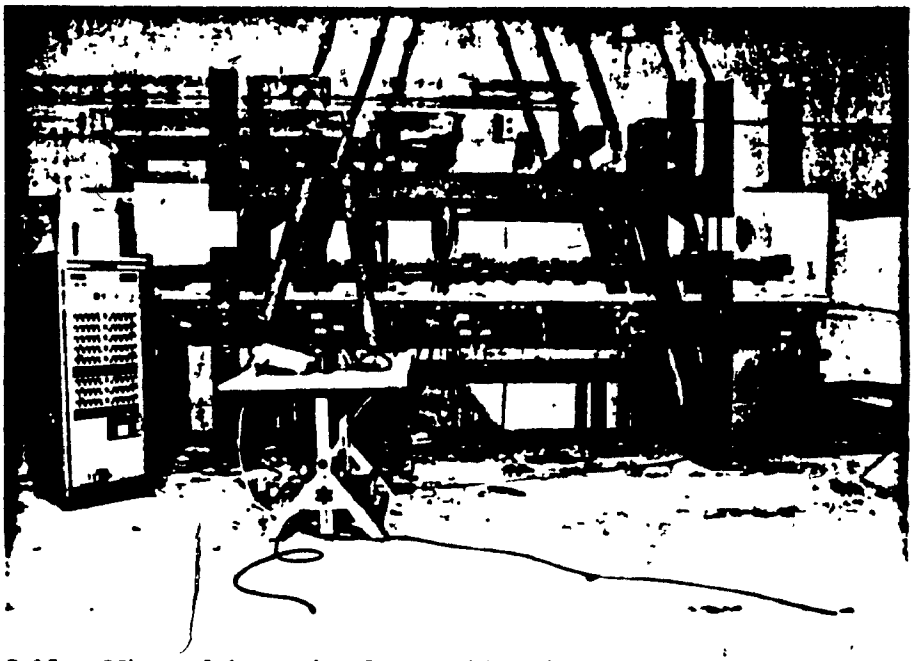

FIG. 3.10 :- View of the testing frame with a girder prepared for test under it.

3.6 - INSTRUMENTATIONS

A) STRAIN MEASUREMENTS :

This was done by means of electric strain gaugesof 8 mm long. The strain gauges were placed in position before casting the concrete for poststressed composite model. In case of prestressed composite model the strain gauges were connected before applying

force. Fig. 3.11 shows an example of electric strain gauges connected to the beam. Cable deformation was measured by a mechanical dial gauge mounted on a specially designed instrument as shown in Fig (3.12).

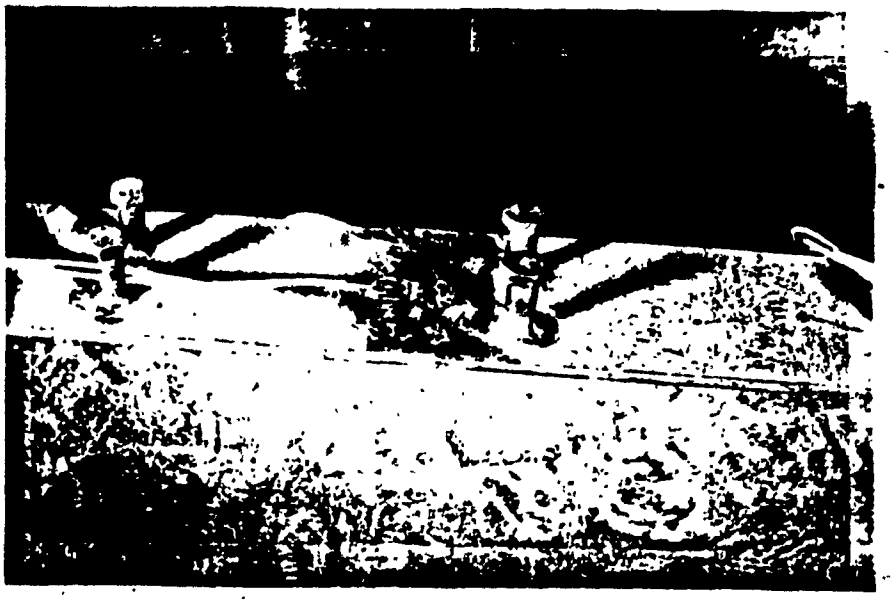

FIG3.11 :-Section where three electric strain gauges are connected to the steel beam.

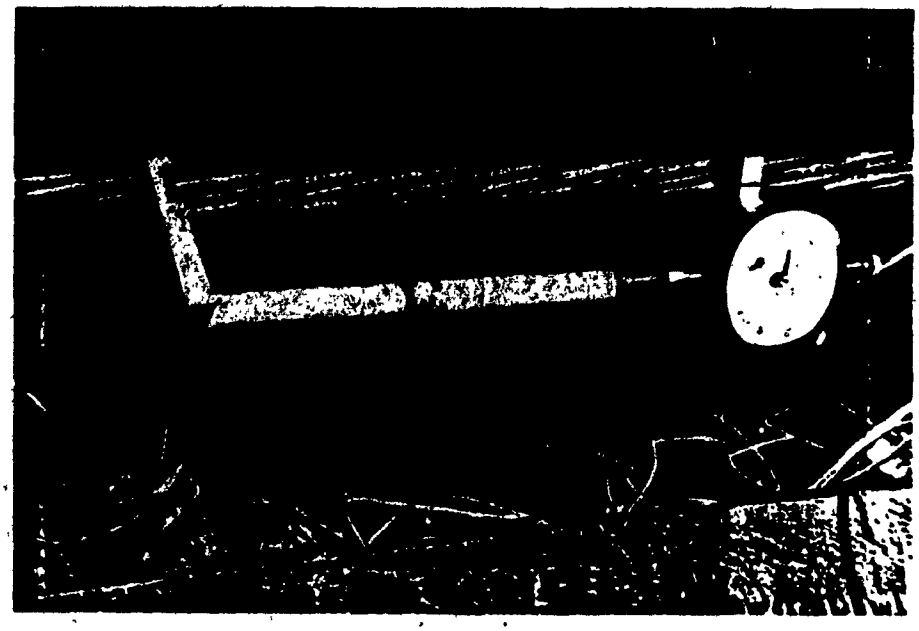

FIG. 3.12 :- Standard dial gauge mounted on an 8" device used for measuring cable elongation.

B) DEFLECTION MEASUREMENT :

This was done by means of mechanical dial gauges mounted to a fixed stand The accuracy of the measurment was 0.001 Ins.Two views of such arrangement are shown in Fig 3.13.

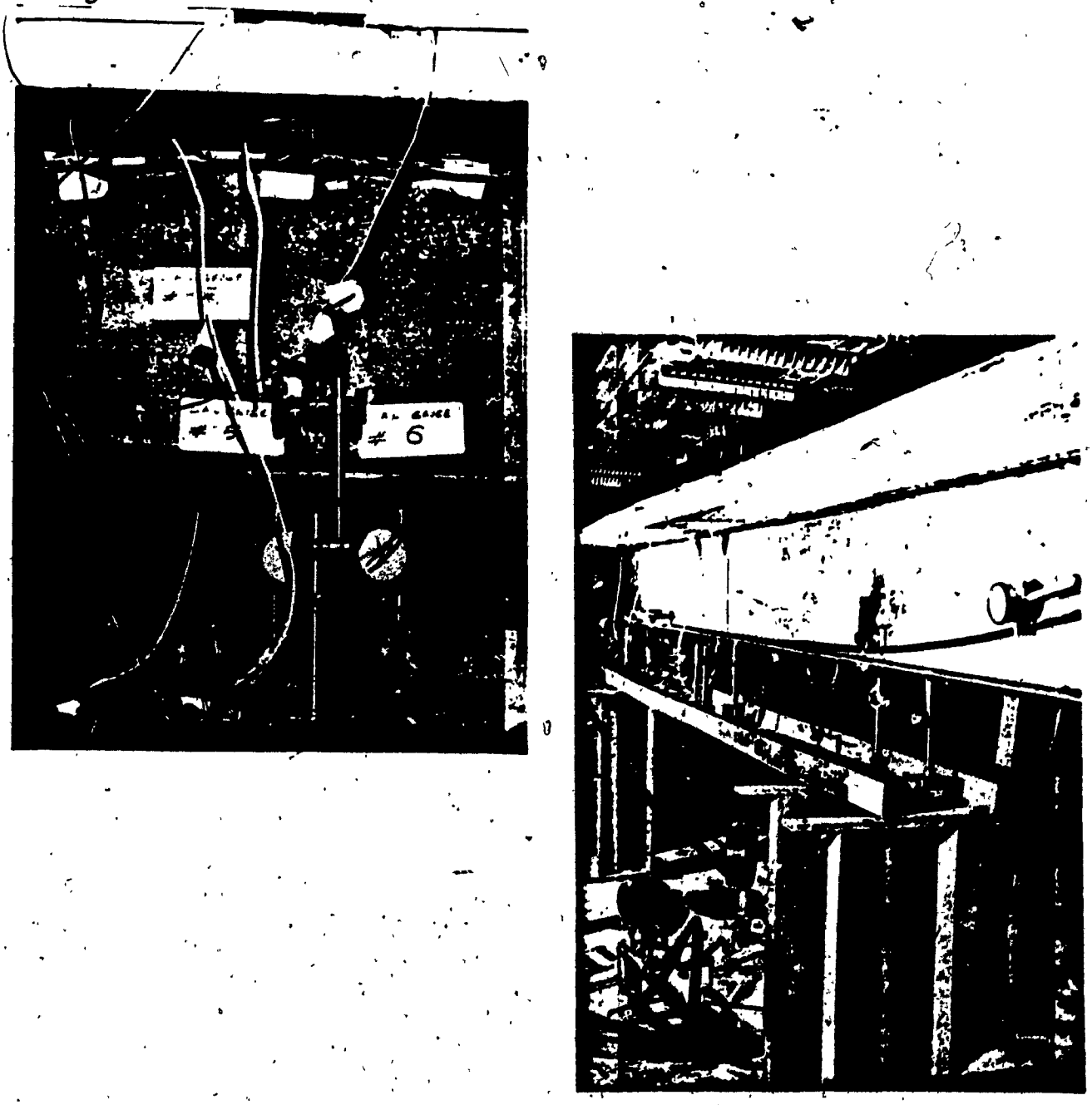

FIG. 3.13:- Dial gauges arrangement to measure deflection along the span.

3.7 -TESTING PROCEDURE:

3.7.1 MODEL " A " :

The steel beam was placed on the supports under the testing frame with 36 electric strain gauges connected at 9 different sections along the span, fresh concrete was then poured on the top flange and cured for 28 days to obtain the required strength. At the end of 28 days 9 additional electric strain gauges were connected to the concrete slab at the top and 11 mechanical dial gauges were fixed under the beam to measure deflection. The following testing procedure was as follows.

TEST # 1:- Poststressed composite girder with bent-up tendon.

The poststressing force was applied by means of two high strength seven wire strand -3/8in dia bent-up tendons passing over two pulleys saddles. These tendons were anchored at one end and pulled from another end. Both tendons were stressed simultaneously with tow jacks on different ends.

The poststressing forces were applied at incremental stages of 4.0, 7.5 , 10.5 , 14.0 , 17.5 and 21.0 KIPS ;this test was repeated three times and measurements were taken at each time. At the end of the 3rd test, while the 21 KIP force (poststressing design force) was applied, a uniformly distributed superimposed dead load of magnitude 0.121 KIP/FT was applied to the girder. The same procedure was repeated three times.

While the superimposed dead load was applied on the girder. The similitude live load (truck load) was applied by means of two hydraulic jacks connected to the testing frame. This part of the test was repeated two more times.

Finally, all loads were removed from the girder in the opposite order of loading and the initial reading was checked.

TEST # 2:- Poststressed composite girder with straight tendon.

The bent-up tendons of the first test were replaced by straight tendons (seven wire strand -3/8ins dia) with constant eccentricity from the neutral axis of the composite girder. The procedure of the tests conducted are in identical manner to test # 1.

3.7.2 MODEL " B " :

In model "B", the steel beam was placed on the supports under the testing frame, after connections of 49 electric strain gauges, 9 mechanical dial gauges were fixed under the beam. Prestressing force was then applied through two straight tendons placed near the bottom flange. Following are details of tests conducted on this model.

Test #1:- Prestressed composite girder with straight tendon. (Lt = L)

The prestressing force was applied by means of two high strength tendons (seven wire strand - 5/8 ins dia) anchored at one end and pulled from the other end simultaneously.The prestressing forces were applied at incremental stages of 4.0, 7.5, 10.5, 14.0, 17.5, and 21.0 KIPs, the same test was repeated two times and measurements were taken at each stage.

At the end of the 2nd test while the 21.0 KIP force (prestressing design force) was applied to the steel beam, the fresh concrete was then poured on the top flange and cured for 28 days. At the end of the curing period, the similitude truck loading was applied to the composite beam. This part of the test was repeated three times and the measurements were taken at each stage.

Test # 2:- Poststressed composite girder with short straight tendon. (Lt < L)

For this test the two straight tendons of the first test were replaced with one short straight tendon (Lt<L) placed symmetrically with respect to web under the bottom flange at the middle part of the span. The poststressing force was applied through the cable in the same increments as in test # 1. The same test was repeated twice and measurements were taken at each stage.

While the 21.0 KIP (poststressing designed force) was applied to the composite beam, the similitude truck loading was applied three times and measurements were taken each time.

CHAPTER 4

TESTS RESULT AND COMPARISON

4.1 - POSTSTRESSED COMPOSITE GIRDER:

During the placing of concrete for the poststressed composite girder, the steel beam was not supported at any points other than that of the two supports at the ends. The dead load was carried by the steel beam only and there were no stresses in the concrete slab. The shrinkage stresses which occured during the hardening of concrete were neglected in this study..

According to the design of the prototype and the model, the eccentricity of the tendon from the neutral axis of the composite section was over the e_{max} limit value (See section 2.6), and as a result some tensile stress was produced in the concrete slab during poststressing. After concrete was cured for 28 days, electric strain gauges were connected to the concrete slab at the top to measure the strains developed by the poststressing force and by the live load.

For comparing experimental results with those predicted by theory, graphs were produced as explained in the following sections.

4.1.1 Test Results and Analysis for Poststressed Composite Girder with BENT-UP Tendon Configurations.

Two tendons were placed on two sides of the steel section and passed over two pulleys as shown in Fig. 4.1. Distribution of stresses at the top fiber of concrete is shown in Fig. 4.2. The poststressing force introduced small tensile stress at the top fiber of concrete at a distance from the beam ends. In the area between the pulleys, there is a small drop in stress level which is probably due to the following reasons :

a) There is a stress concentration near the pulleys, which causes higher stresses than other sections.

b) Between the two pulleys, the girder acts locally as a two points supported beam (supported at pulley connection).Therefore the beam self weight in the middle produced opposite stresses to those produced by poststressing and stresses of the same sign over pulleys.

The poststressing force is subjected to a losses due to some friction at direction change of tendon over pulley points, therefore the stresses between pulleys are smaller than the theoretical value.

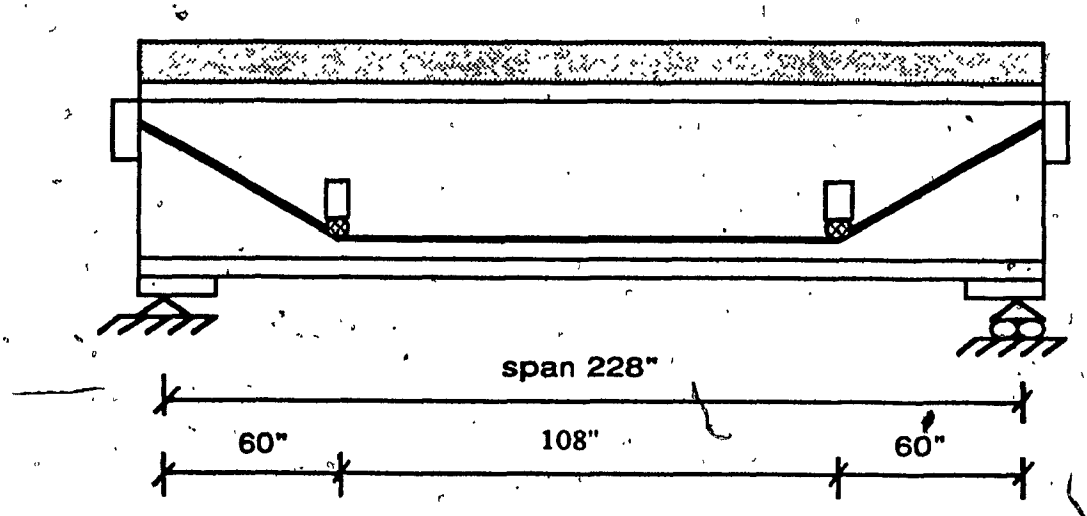

BENT-UP TENDON ARRANGEMENT

FIG. 4.1

The theoretical values in Fig (4.2) were calculated using basic Equation 4.1. where e_{cp} is the only variable in calculating the stresses along the span.

$$\sigma_c^t = \frac{1}{n}\left[-\frac{P}{A_{cp}} + \frac{P e_{cp}}{S_{cp}^t}\right] \qquad (4.1)$$

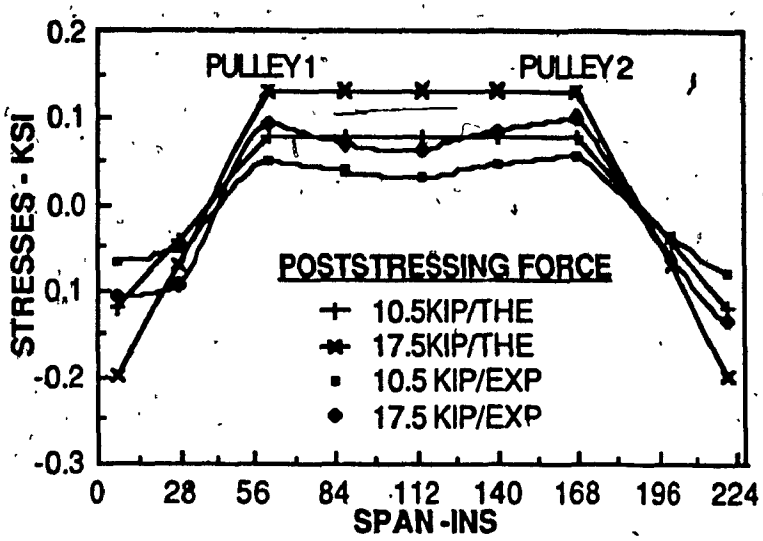

FIG 4.2: BENTUP TENDON. Stress variation at the top of concrete slab.

Stresses developed along the span at the top fiber of steel under the poststressing application for the bent-up tendon are shown in Fig 4.3 . The stress variation follows the tendon configuration along the span in the reverse manner.

Fig 4.3 also shows the comparison of stresses developed at the top fiber of steel along the span under poststressing application. Theoretical values were calculated using Equation 4.2.

Since the tendons were placed near the top flange at the beam ends, the experimental values at that location are higher than the calculated value, and that is because the effect of poststressing force reaches the top flange immediately after the anchorage at the end(see section 4.4).

$$\sigma_s^t = -\frac{P}{A_{cp}} + \frac{P \cdot e_{cp}}{S_{cp}^{Ls}} \qquad (4.2)$$

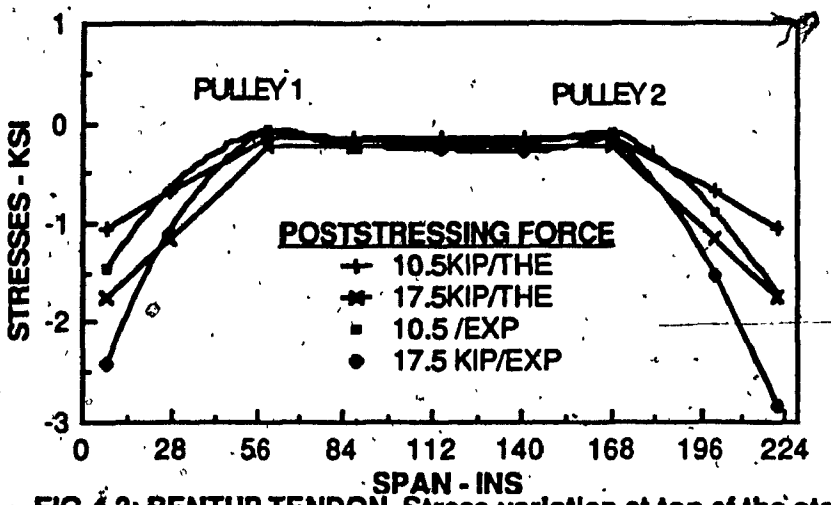

FIG 4.3: BENTUP TENDON. Stress variation at top of the steel beam.

Stresses developed along the span at the bottom fiber of concrete under poststressing application are shown in Fig (4.4). The stress variation along the span followed the tendon configuration along the span. The same reasons a & b are applicable for the reduction of stresses between the pulleys.

Fig (4.4) also shows the comparison of stresses developed at the bottom fiber of steel under poststressing application and the theoretical values were calculated using the basic Equation 4.3.

$$\sigma_g^b = -\frac{P}{A_{cp}} - \frac{Pe_{cp}}{S_{cp}} \qquad (4.3)$$

The upward deflection at mid span measured under poststressing application are shown in Fig 4.5. The theoretical values was calculated using Equation 4.4. The experimental value are smaller than the theoritical value , for this reason the actual

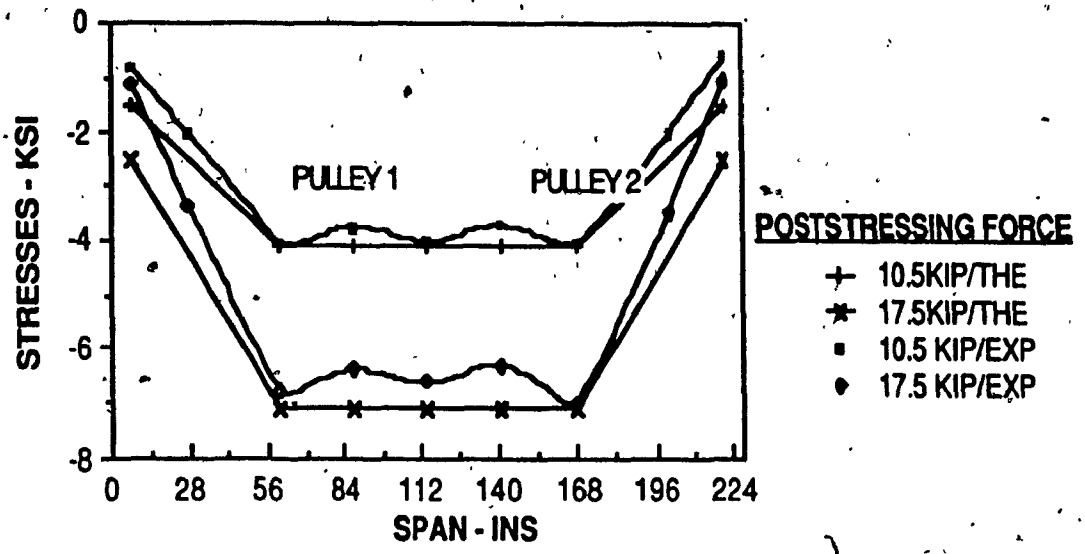

FIG 4.4: BENTUP TENDON. Stress variation at bottom of the steel beam.

computed deflection should be modified to accomodate the losses, or in equation 4.4, instead of poststressing force (P), the value (P - losses) should be used to obtain actual deflection.

$$\delta_{max}^{bu} = -\frac{P.e}{24\,EI_{cp}}\,(3L^2 - 4a^2) \qquad (4.4)$$

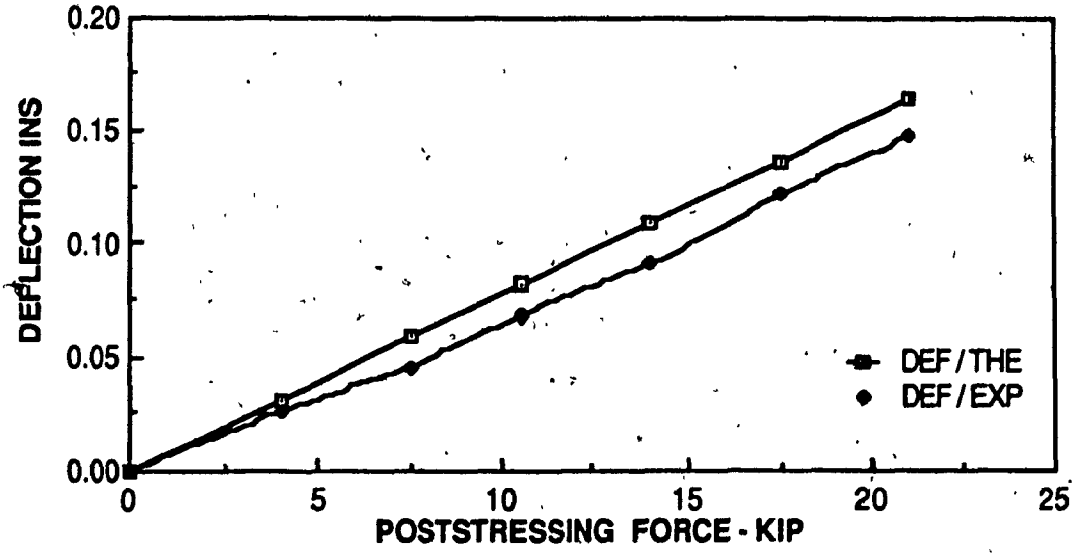

FIG 4.5: BENTUP TENDON. Deflection at mid span.

4.1.2 - Test Result and Analysis for Poststressed Composite Girder with STRAIGHT Tendon Configuration .

A tendon was placed on each side of the steel section at a constant eccentricity from the neutral axis of the composite section as shown in Fig (4.6).

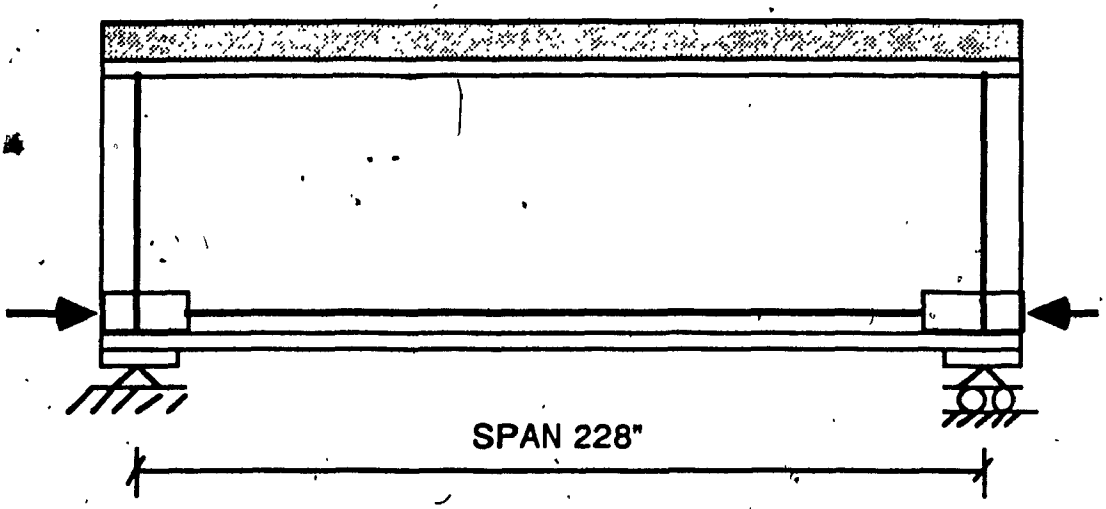

STRAIGHT TENDON ARRANGEMENT

FIG.4.6

Fig (4.7) shows the stresses developed at the top fiber of concrete along the span under the poststressing force. The theoretical values in the Fig (4.7) are calculated using basic Equation (4.1).

The tensile stress produced by the poststressing force at the top fiber of concrete dose not follow a straight line pattern as given by Equation 4.1. This effect reaches to the top fiber of concrete at a distance of approximately 3 to 4 times the section depth from the beam ends(End block effects, section 4.4). For this reason, Equation 4.1 can not be used to calculate the stresses developed in top fiber of concrete at a distance less than 4 times depth (section) from the beam ends.

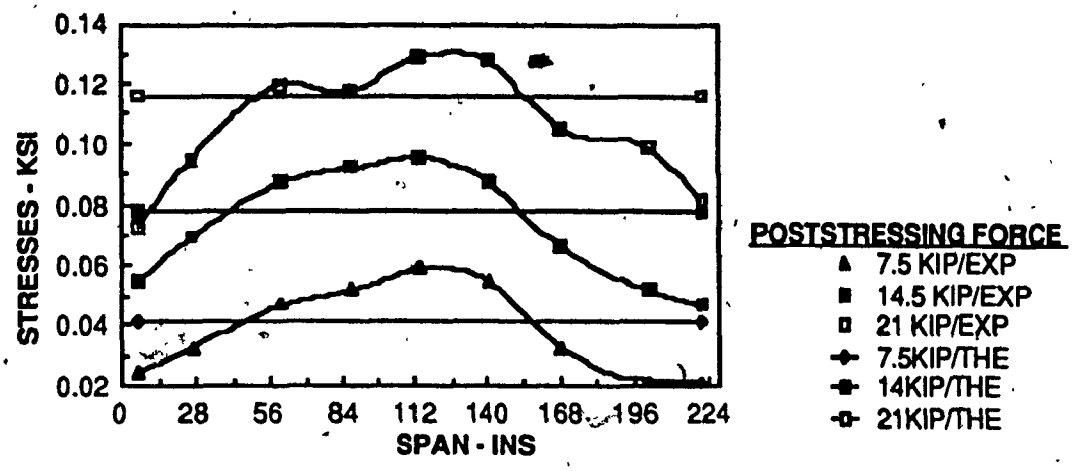

FIG 4.7: STRAIGHT TENDON. Stress variation at top of the concrete slab.

Close observations showed no cracks on the top of concrete under the design poststressing force (21 KIPS).

Fig (4.8) shows the stresses measured at the top fiber of the steel under the poststressing application along the span. The theoretical values were calculated using Equation (4.2). This equation also can not be used to calculate the stresses under poststressing application near the beam ends at the top fiber of steel.

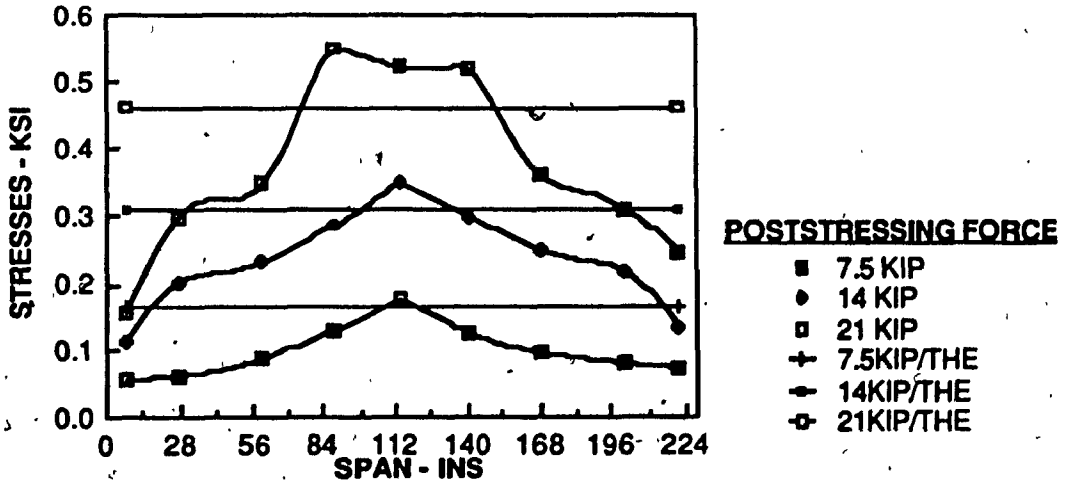

FIG 4.8: STRAIGHT TENDON. Stress variation at top of the steel beam.

Fig(4.9) shows the stresses developed along the span at the bottom fiber of the steel section under the poststressing application. In this case the tendons are very close to the bottom flange, so that the effect of the poststressing force reaches to the bottom fiber immediately after the supports. The theoretical values were calculated using Equation 4.3. The experimental values and theoritical values are very close to each other (End block effect, section 4.4).

Fig (4.10) shows the upward deflection at mid span measured by the straight tendon under poststressing application . The theoretical values at the mid span were calculated using Equation (4.5). In this case also the experimental values are smaller than theoritical values, and hence the deflection calculated by Equation 4.5 has to be modified to obtain actual deflection.

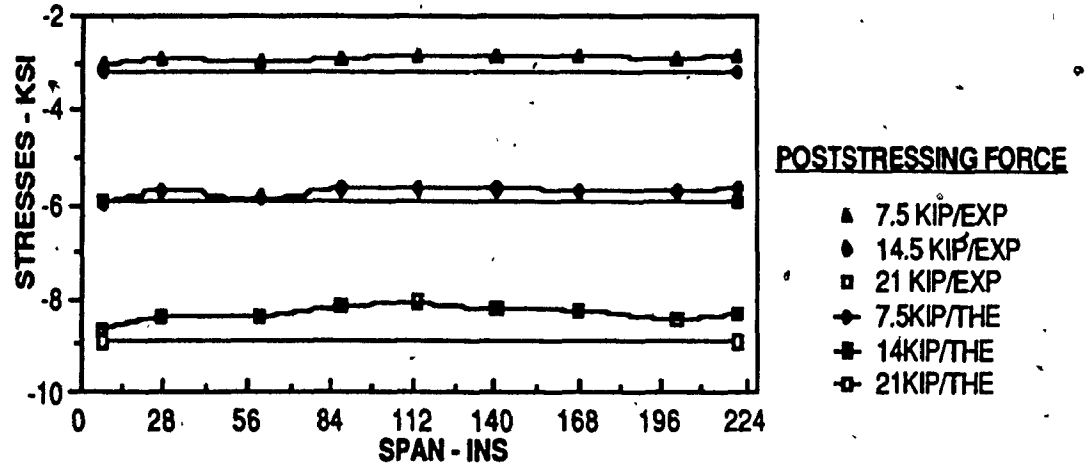

FIG 4.9: STRAIGHT TENDON. Stress variation at the bottom of steel beam.

$$\delta_{max}^{po} = -\frac{P e_{cp} L^2}{8EI_{cp}} \qquad (4.5)$$

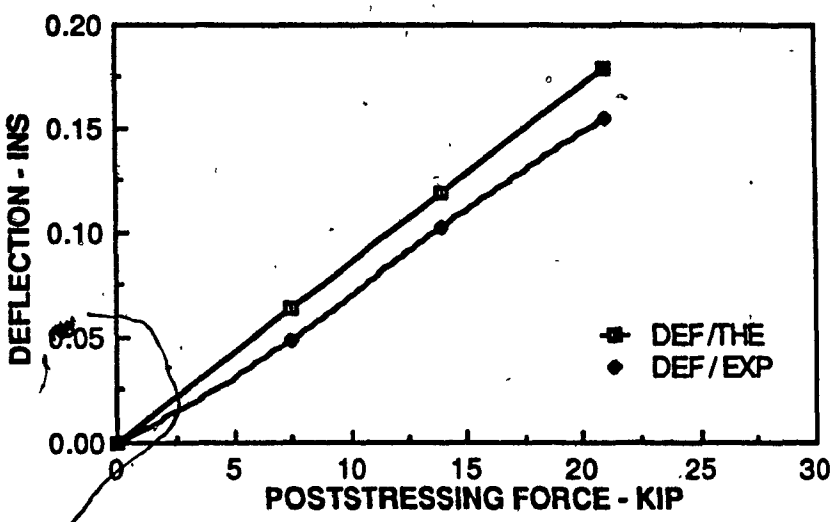

FIG 4.10: STRAIGHT TENDON. DEFLECTION AT MID SPAN

4.1.3 Test Result and Analysis for Poststressed Composite Girder with SHORT STRAIGHT Tendon Configuration.

In this case, as it is shown in the Fig 4.11, a straight tendon was placed at mid span of the girder 60 Inches from each end, and the poststressing force was applied by means of a hydraulic jack from one end, while the other end was fixed by a friction anchor chock.

Fig 4.12 shows the stress variation at top fiber of steel under the poststressing application. The sudden increment of stresses observed at the anchor points are due to concentration of stresses. Observation from previous tests (bent-up and straight tendon configuration) shows that the stresses normally followed the dotted line indicated in Fig 4.12. However, due to the location of anchor block (being at a distance away from the beam supports), a certain amount of stress concentration was added to the overall stress level in the vicinity of anchor connection to the beam as shown in Fig 4.12.

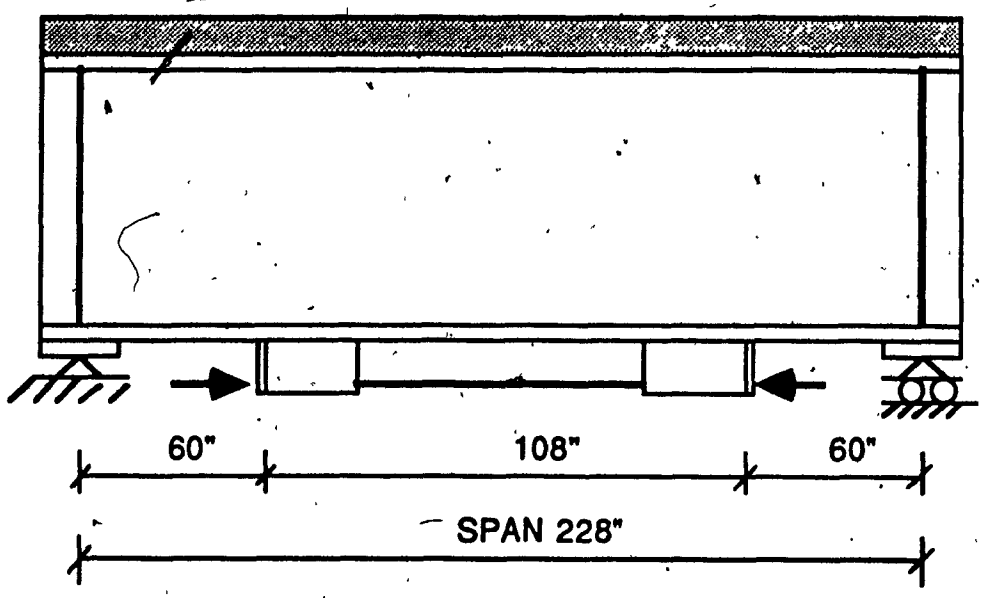

INSIDE STRAIGHT TENDON ARRANGEMENT

FIG 4.11

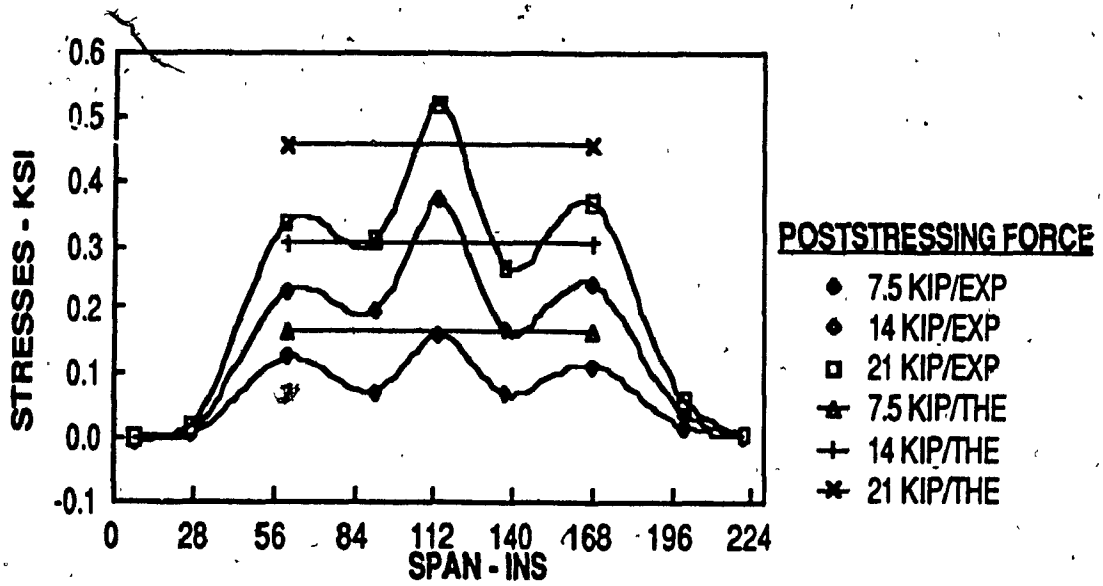

FIG 4.12: SHORT STRAIGHT TENDON. Stress variation at top of the steel.

Stress variation along the span at bottom fiber is shown in Fig 4.13. The maximum stress values were reached at a very short distance from the anchor points. This is mainly due to the relatively close location of the cable from the bottom flange (End block effects,section 4.4).

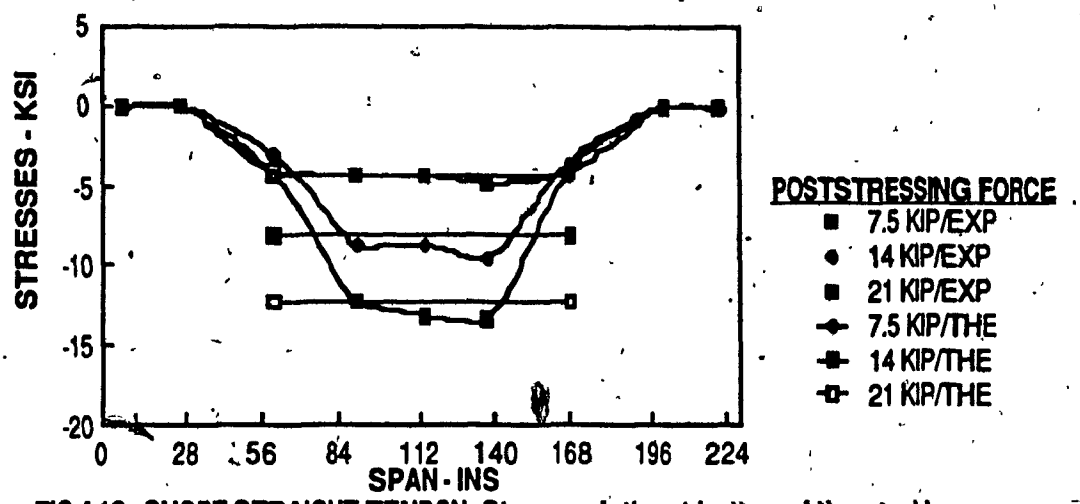

FIG 4.13: SHORT STRAIGHT TENDON. Stress variation at bottom of the steel beam.

4.2 - PRESTRESSED COMPOSITE GIRDER

The steel section (W 310 X 24) was placed in position over the supports and after the connection of electric strain gauges and mechanical dial gauges to the steel beam, the prestressing force was applied to the steel beam through two straight tendons placed near the bottom flange as shown in Fig 4.14.

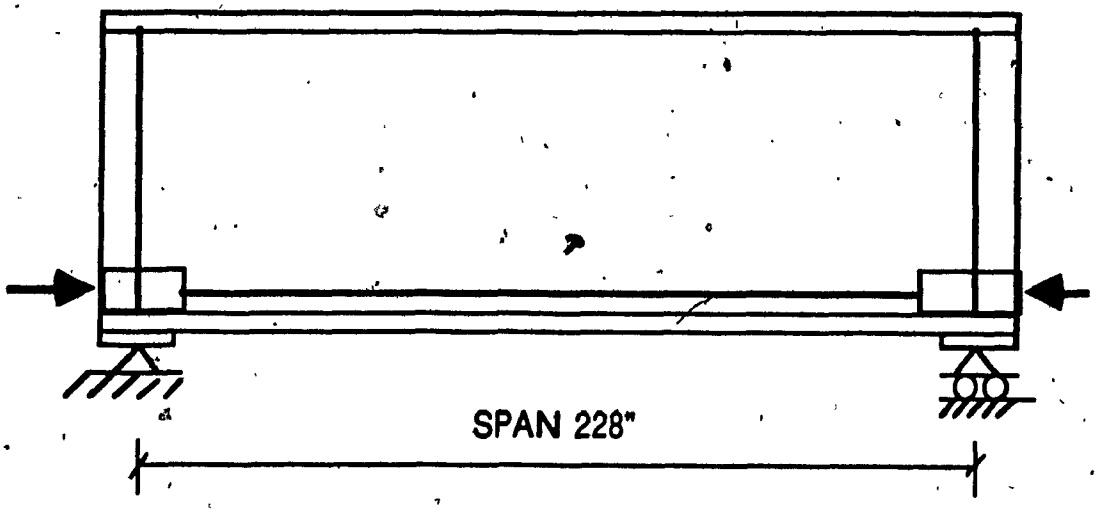

STRAIGHT TENDON ARRANGEMENT

FIG 4.14

4.2.1 - Test Results and Analysis for Prestressed Composite Girder with STRAGHT Tendon Configuration.

Fig 4.16 shows the stresses developed at the top fiber of steel under prestressing application (only steel section). The recorded stresses at mid span are very close to the calculated values by Equation (4.2) However, near the beam end, the concentration of stresses resulted in an increase of stress level as shown in Fig 4.16.

Fig (4.17) shows the stresses developed at the bottom fiber of the section. and since the cable was placed very close to the bottom flange, the prestressing force effect reaches this fiber immidiately after the end block. The shown results are very close to the theoritical value predicted by Equation (4.2).

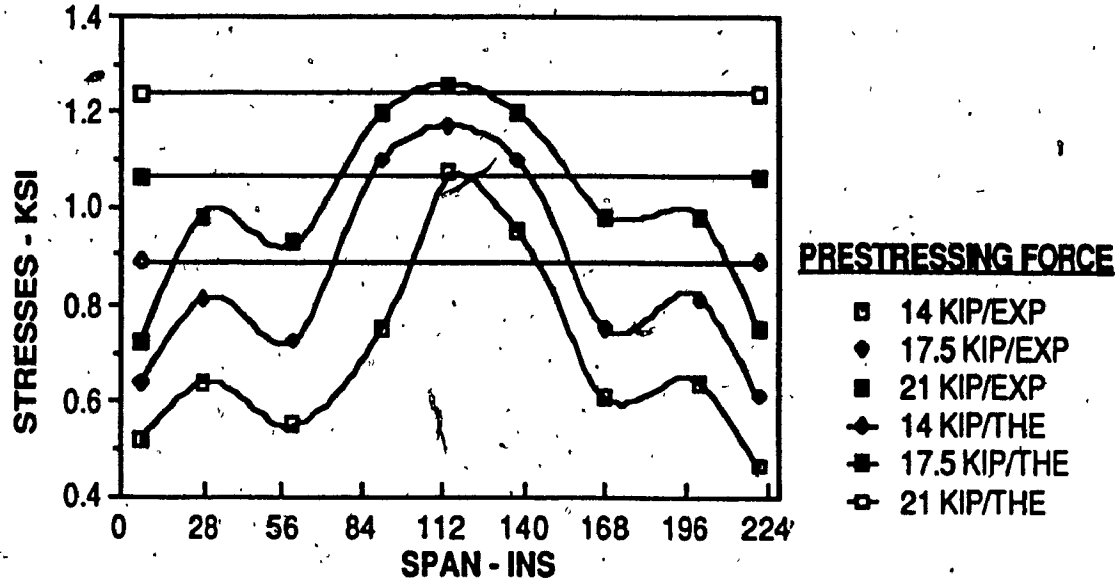

FIG 4.16: STRAIGHT TENDON. Stress variation at top of the steel beam.

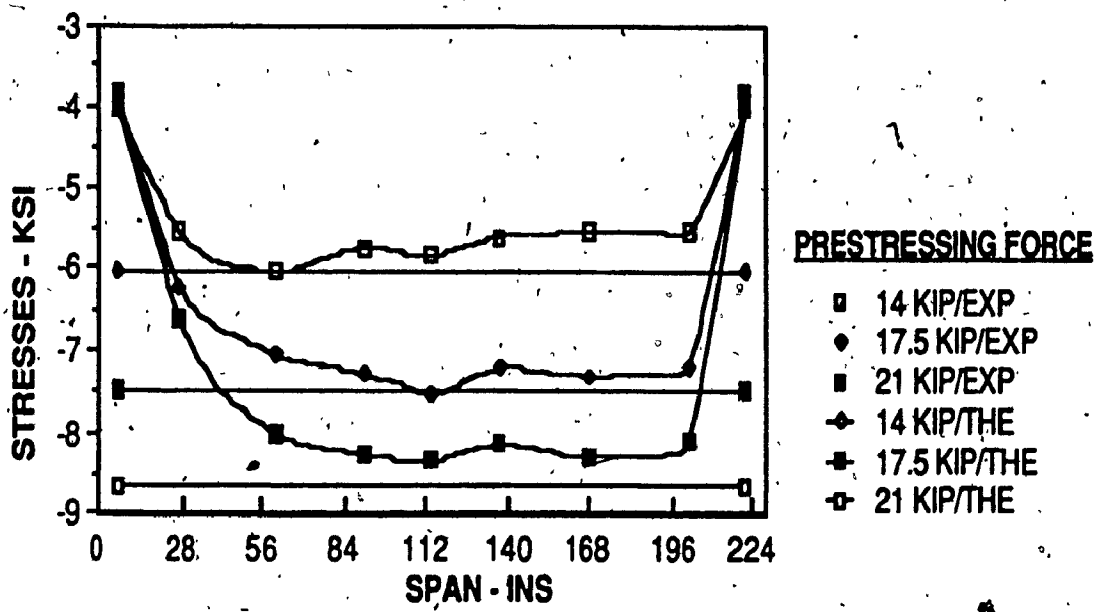

FIG 4.17: STRAIGHT TENDON. Stress variation at bottom of the steel beam.

The experimental values for the deflections were measured by means of mechanical dial gauges, and shown in Fig 4.18. The experimental values are not very close with the theoritical values calculated by Equation (4.5). As in previous sections, a modification in actual deflection computation should be applied.

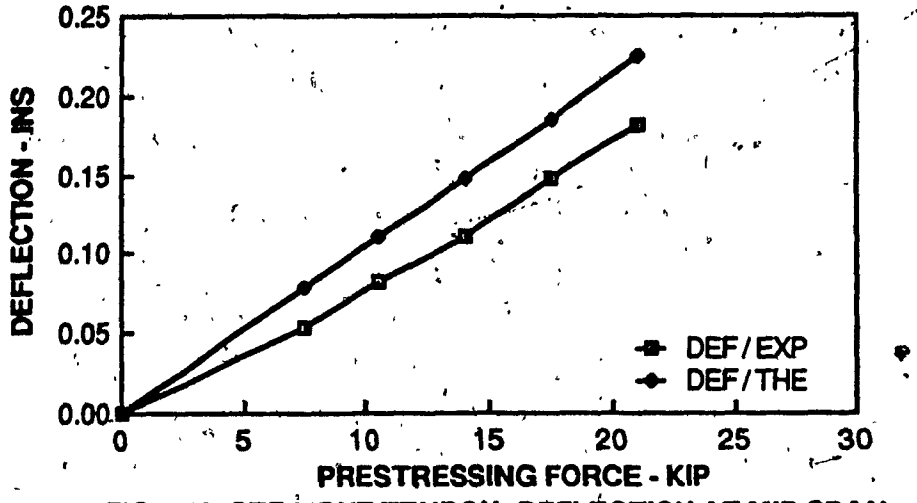

FIG 4.18: STRAIGHT TENDON. DEFLECTION AT MID SPAN.

4.3 Increment in Initial Tendon Force Under Application of External Load.

The cable elongation under the application of external load was measured experimentally by means of mechanical dial gauges mounted on a special clamp designed for this purpose(See section 3.6-A).

The magnitude of super imposed dead load(uniformly distibuted) was very small, hence the increment in initial tendon force was also small. The experimental readings of such small elongation were not possible, where as in the case of live load (truck loading) it was found that this increment in tendon force had a considerable value.

Tables(4.1, 4.2,& 4.3) show the comparison of the increment in initial poststressing force under application of live load (truck loading) for bentup tendon, straight tendon and short straight tendon respectively.

INITIAL POSTSTRESSING FORCE	CROSS SECTION AREA OF TENDONS	ECCENTRICITY FOR THE TENDON	INCREMENT CALCULATED USING EQUA. 2.13	INCREMENT MEASURED BY THE EXPRIMENT
21 KIP	2 X .08 IN^2	8.26 IN	1.429 KIP	1.389 KIP

TABLE 4.1:- BENTUP TENDON. POSTSTRESSING FORCE INCREMENT DUE TO TRUCK LOADING

INITIAL POSTSTRESSING FORCE	CROSS SECTION AREA OF TENDONS	ECCENTRICITY FOR THE TENDON	INCREMENT CALCULATED USING EQUA. 2.16	INCREMENT MEASURED BY THE EXPRIMENT
21 KIP	2 X .215 IN^2	8.26 IN	3.209 KIP	3.187 KIP

TABLE 4.2 :- STRAIGHT TENDON. POSTSTRESSING FORCE INCREMENT DUE TO TRUCK LOADING

INITIAL POSTSTRESSING FORCE	CROSS SECTION AREA OF TENDONS	ECCENTRICITY FOR THE TENDON	INCREMENT CALCULATED USING EQUA. 2.13	INCREMENT MEASURED BY THE EXPRIMENT
21 KIP	2 X .215 IN^2	12.889 IN	5.497 KIP	5.444 KIP

TABLE 4.3 :- SHORT STRAIGHT TENDON. POSTSTRESSING FORCE INCREMENT DUE TO TRUCK LOADING

4.4 End Block Effect :

The portion of a prestressed/poststressed member surrounding the anchorages of the tendon is often termed the end block. Throughout the length of the end block, the tendon force is transferred from almost a concentrated area and distributed through the entire beam section. The theoretical length of the end block (transmission length) is the distance through which this change takes place[5].

A large force applied to the end of a prism, such as show in Fig 4.19, results in principal compressive stresses that follow a pattern similar to the solid lines and principal tensile stresses that follow along line similar to the dashed line. In a simple prismatic beams at a distance of about one times the depth of the block from the end, the stresses are approximately equal the value that would be computed from the usual combined stress relationship [4].

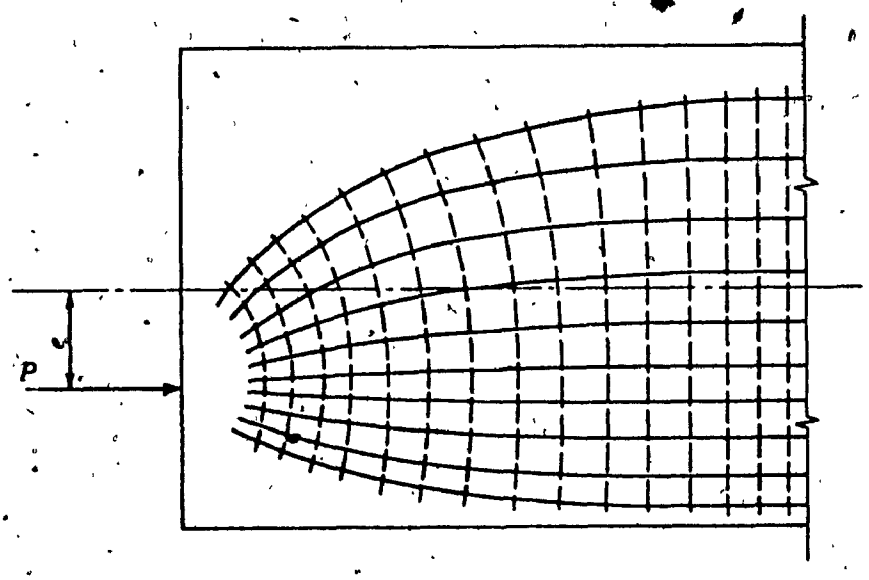

Fig 4.19 Approximate Paths of Principal Tensile and Compressive Stresses in a Prism that is Eccentrically Loaded

Recorded data obtained from the experiment showed that in composite beams the distribution of principal stresses did not follow the normal stress flow pattern of a simple prismatic beam shown in Fig 4.19. It was also observed that the transmission lenght for stresses measured along the span at the top fiber could reach the values of three to five times the section depth depending on tendon configuration and eccentricity. In addition, for stresses along the bottom fiber of the beam, the transmission length was less than one time the section depth.

CHAPTER 5

SUMMARY AND CONCLUSION

5.1 SUMMARY

The present study deals with the behavior of prestressed and poststressed composite girders and include model test and analysis. The research work emphasized on the stress distribution along the span across the section, upward deflections under prestressing and poststressing effects and the increment in initial tendon force under external loads. The loads which are considered in this study includes dead loads, superimposed loads, prestressing or poststressing forces and live loads with impact effect.

Since most of the literature dealt with prestressed or poststressed composite girders, this research study dealt with both prestressed and poststressed composite girders.

The experimental work was conducted on two quarter-scale models. A total number of fourty eight tests were conducted. Mechanical properties of steel girders were verified based on tests on cut-out pieces from the web and flange. The compression strengths of concrete was checked at different curing ages. The mechanical properties of stressing cables used in this experimental work were specified by supplier -Supreme Inc.

Formulas used for analysis were developed or improved to predict the stresses developed along the span, upward deflections and increment in initial tendon force.

The effects of losses caused by creep, shrinkage and tendon relaxation together with residual stresses in the steel beam were not considered.

5.2 CONCLUSIONS

The following conclusions can be drawn based on the research work performed:

1. The prestressing and poststressing of a composite section using high strength tendon significantly improves the stress (65% to 85% of the allowable compression stress at bottom fiber) along the span and across the sections.

2. The method of analysis presented for prestressed and poststressed composite beam gives a reasonable approximation for the stresses near the midspan (a critical section).

3. If an exact analysis is required for the stresses near the beam ends, significant effect of end block has to be considered.

4. Consideration should be given in design of bracket (bearing arrangement for tendon) at the attachment points of tendon to the steel beam.

5. The stresses at the top fibre of steel are not significantly affected by the poststressing force. This is due to the location of the neutral axis of composite section, which is near the steel top flange. For economy reasons, it might be advisable to provide prestressing before casting of concrete (prestressing).

6. There is no significant difference in the final tensile stresses developed along the bottom fibre, by prestressing or poststressing of a composite section.

REFERENCES

1. Abbott, P.A., " Simply Supported Steel I-Beams Prestressed with Horizontal Restrained Tendons", Thesis presented to Rice University, Houston, Texas, in partial fulfillment of the requirements for the degree of Masters of Engineering, 1963.
2. Czarnota-Bojarski, Roman, "Vorgespannte Stahl Trager Statische Berechnung", Berlashgesllschaft Rvdolf Muller Koln-Bravnsfeld, 1957.
3. Hoadley, P.G., "Behaviour of Prestressed Composite Steel Beams", Journal of the Structural Division, ASCE, June, 1963, pp. 21-34.
4. Libby, J. R., "Modern Prestressed Concrete", Van Nostrand Reinhold Company, New York, Third Edition, 1984.
5. Lin, T. Y., "Design of Prestressed Concrete Structures", John Wiley & Sons Inc., New York, Second Edition, 1970.
6. Reagan, Roald S. "An Analytical Study of the Behaviour of Prestressed Compostie Beams", Thesis presented to Rice University, Houston, Texas, in partial fulfillment of the requirements for the degree of Masters of Engineering, 1966.
7. Strass, J.C., "An Experimental and Analytical Study of Prestressed Composite Beams", Thesis presented to Rice University, Houston, Texas, in partial fulfillment of the requirements for the degree of Masters of Engineering, 1964.
8. Szilard, R. "Design of Prestressed Composite Steel Structures", Journal of the Structural Engineering Division, ASCE, Nov., 1959, pp. 97-123.
9. Tachibana, Y.; Kondo K. and Ito, K., "Experimental Study on Composite Beams Prestressed with Wire Cables", Symposium on the Use of High Strength Steel Structures, Japan Society for the Promotion of Science, Tokyo, May, 1963.

APPENDIX "A"

MODEL ANALYSIS

- Span — 19 ft.
- Super imposed Dead Load — 121 k/ft
- Live Load
  Similitude Truck Loading According to MS-250-77

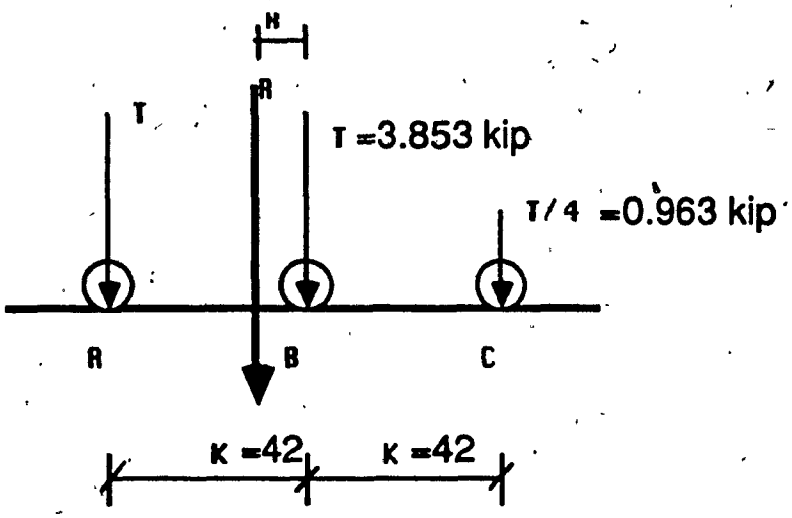

FIG. A-1:- SIMILITUDE MS-250-77 TRUCK LOADING

- Poststressing and Prestressing Force (Assume straight tendon along the span) — 21 KIPS
- **Section Properties:**
- Steel Section — W310x24
- fy — 44 KSI
- A_s — 4.71 in.
- E_s — 29×10^3 KSI
- Concrete slab thickness — 2 in.

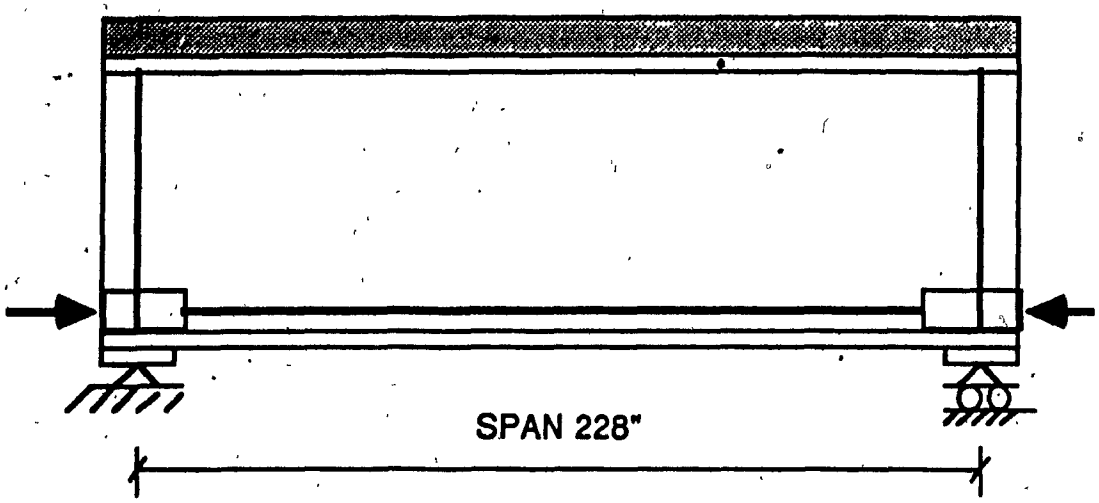

FIG. A-2:- CABLE CONFIGURATION ALONG THE SPAN

- Effective width of slab — 18 in.
- Model A — $f_c' = 3.9$ KSI; $E_c = 3.564 \times 10^3$ KSI; $n = 8.137$
- Model B — $f_c' = 3.87$ KSI; $E_c = 3.545 \times 10^3$ KSI; $n = 8.285$

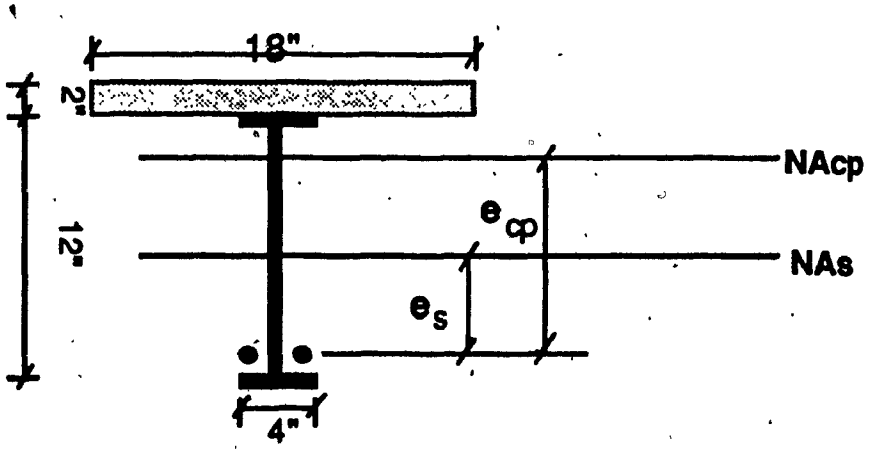

FIG. A-3:- CROSS SECTION OF COMPOSITE GIRDER

- Assumed n ratio to be constant for both model	$n = 8.137$
- Area of the transformed composite section	$A_{cp} = 9.13\ in^2$
- Eccentricity of the tendon from neutral axis of the composite section	$e_{cp} = 8.26$ in.
- Eccentricity of the tendon from neutral axis of the steel section only.	$e_s = 4.871$ in.
- Cross section area of the tendon	$A_{cb} = 2x\ 0.215\ in^2$
- $0.7\ f_{pu}\ A_{cb}$	37.6 KIPS
- I_s	$103\ in^4$
- I_{cp}	$216.2\ in^4$
- W_s	16 lb/ft
- W_c	35 lb/ft
- $Y_s^t = Y_s^b$	6 in
- Y_{cp}^t	4.611 in.
- $Y_{cp}^{t.s}$	2.611 in.
- Y_{cp}^b	9.389 in.
- $S_s^t = S_s^b$	$17.166\ in^3$
- S_{cp}^t	$46.88\ in^3$
- $S_{cp}^{t.s}$	$62.80\ in^3$
- S_{cp}^b	$23.026\ in^3$

- **MOMENTS AT MID SPAN**

M_s	8.664 K-in
M_c	18.95 K-in

Using equation (2.8)

$$M_{mid} = T\,(0.5625\,L - 0.8334\,K - 0.062K^2/L) \qquad (2.8)$$

M^{LL} 357.43 K-in.

- **MOMENTS UNDER POINT LOAD B OF THE TRUCK**

Using equation (2.4)

$$M_D = M_B = q\,(0.125\,L^2 - 0.0137K^2) \qquad (2.4)$$

M_s	8.6317 K-in.
M_c	18.88 K-in.

Using equation (2.7)

$$M_{Bt} = M_{max} = T(0.5625L - 0.625K + 0.062K^2/L) \qquad (2.7)$$

M^{LL} 394.85 K-in.

Therefore the critical section which has to be studied is the section under point load B.

1) PRESTRESSED COMPOSITE SECTION

- Stress due to self weight of steel

$$\sigma_s^t = \sigma_s^b = \pm 0.504 \text{ KSI}$$

- Stresses due to prestressing force.

$\sigma_s^t = +1.5$ KSI

$\sigma_s^b = -10.41$ KSI

- Stresses due to concrete weight.

$\sigma_s^t = \sigma_s^b = \pm 1.104$ KSI

- Increment in prestressing force due to concrete weight. using equation (2.17)

$$\Delta P = \frac{qL\, e_{cp}}{12\left[e_{cp}^2 + \frac{I_{cp}}{A_{cp}} + \frac{E_s I_{cp}}{A_{cb} E_{cb}}\right]} \qquad (2.17)$$

$\Delta P^c =$ (negligible) 0.0009 KIPS

- Increment in prestressing force due to superimposed dead load.

$\Delta P^c =$ (negligible) 0.0311 KIPS

- Stresses due to superimposed dead load.

$\sigma_{cp}^t = -0.1735$ KSI

$\sigma_{cp}^{t,s} = -1.042$ KSI

$\sigma_{cp}^b = +2.846$ KSI

- Stresses due to truck loading.

$\sigma_{cp}^t = -1.03$ KSI

$\sigma_{cp}^{t,s} = -6.28$ KSI

$\sigma_{cp}^b = +17.152$ KSI

- Increment in prestressing force due to truck loading using equation (2.16).

$$\Delta P = \frac{Te\ (0.2812\,L^2 - 0.5314\,K^2)}{L\left[e_{cp}^2 + \frac{I_{cp}}{A_{cp}} + \frac{E_s\,I_{cp}}{A_{cb}\,E_{cb}}\right]} \qquad (2.16)$$

$$\Delta_p^T = 3.211 \text{ KIPS}$$

- Stresses due to increment which cause by application of truck loading.

$$\sigma_{cp}^t = +0.026 \text{ KSI}$$

$$\sigma_{cp}^{t.s} = +0.070 \text{ KSI}$$

$$\sigma_{cp}^b = -1.50 \text{ KSI}$$

2) POSTSTRESSED COMPOSITE SECTION

- Stresses due to self weight. of steel

$$\sigma_s^t = \sigma_s^b = \pm 0.504 \text{ KSI}$$

- Stresses due to concrete weight.

$$\sigma_s^t = \sigma_s^b = \pm 1.104 \text{ KSI}$$

- Stresses due to poststressing.

$$\sigma_{cp}^t = +0.172 \text{ KSI}$$

$$\sigma_{cp}^{t.s} = +0.459 \text{ KSI}$$

$$\sigma_{cp}^b = -9.835 \text{ KSI}$$

- Stresses due to truck loading.

$\sigma_{cp}^{t} = -1.03$ KSI

$\sigma_{cp}^{t \cdot s} = -6.28$ KSI

$\sigma_{cp}^{b} = +17.152$ KSI

- Stresses due to increment which is caused by trucking loading.

$\sigma_{cp}^{t} = +0.026$ KSI

$\sigma_{cp}^{t \cdot s} = +0.070$ KSI

$\sigma_{cp}^{b} = -1.50$ KSI

Table A-1 shows the loading sequences for both prestressed and poststressed composite for this example.

TABLE A-1:- Loading Stage

LOADING-STAGE	PRESTRESSED	POSTSTRESSED
1	Steel Weight	Steel Weight
2	Prestressing	Concrete Weight
3	Concrete Weight	Poststressing
4	Super-imposed dead load	Super-imposed dead load
5	Live load and impact	Live load and impact
6	Increment due to live load and impact	Increment due to live load and impact

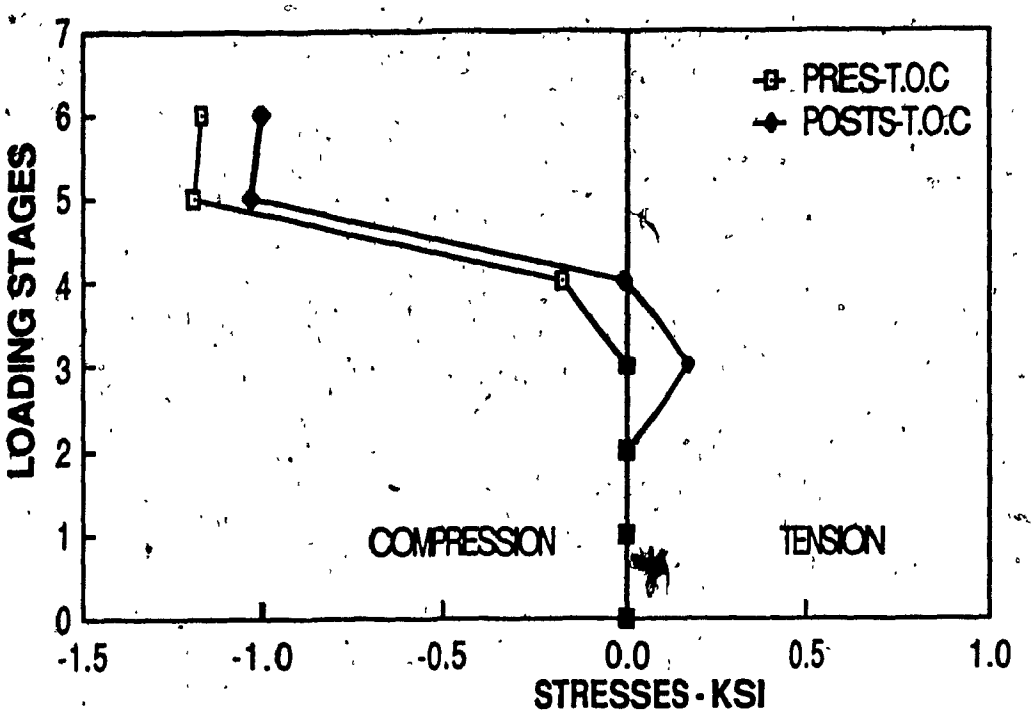

FIG. A-4:- STRESSES AT TOP FIBER OF CONCRETE AT EACH STAGE OF LOADING (REF. TO TABLE A-1)

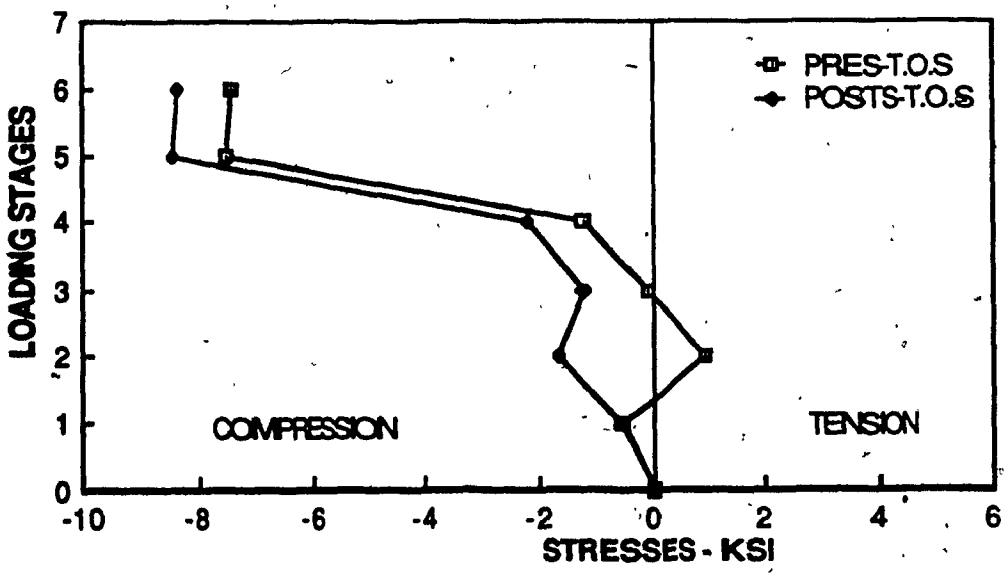

FIG. A-5:- STRESSES AT TOP FIBER OF STEEL AT EACH STAGE OF LOADING (REF. TO TABLE A-1)

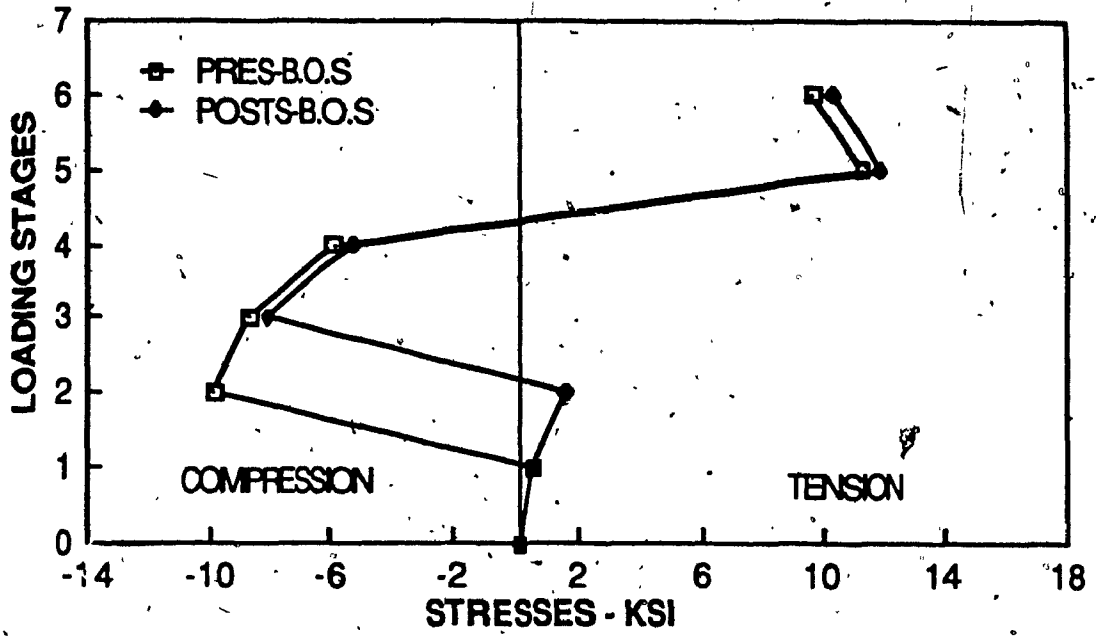

FIG. A-6:- STRESSES AT BOTTOM FIBER OF STEEL AT EACH STAGE OF LOADING (REF. TO TABLE A-1)

DEFLECTION

- Under self weight of the steel section using equation (2.29)

$$\delta^{UDL} = \frac{5\,q\,L^4}{384\,EI} \qquad (2.29)$$

$\delta^s = 0.015$ in..

- under concrete weight using equation (2.29)

$\delta^c = 0.0343$ in

- under super imposed dead load using equation (2.29)

$\delta^{SD} = 0.0565$ in

- Under poststressing force using equation (2.32)

$$\delta^{PR/PO} = -\frac{(P + \Delta P)\,eL^2}{8EI} \qquad (2.32)$$

$\delta^{PO} = 0.179$ in

Under prestressing force using equation (2.32)

$\delta^{PR} = 0.2225$ in

Under truck loading using equation (2.36)

$$\delta_B^T = \frac{T}{3EIL}(A + B + C) \qquad (2.30$$

where

$$A = \frac{1}{4}(0.25L^4 + 0.6327\,K^4 - 3.4205\,K^2L^2 - 0.1666\,KL^3 - 0.7051\,K^3L)$$

$$B = (0.25\,L^2 - 0.0275\,K^2)^2$$

$$C = \frac{1}{16}(0.25\,L^4 + 0.2798\,K^4 - 1.555\,K^2L^2 + 0.336\,K^2L)$$

$\delta^T = 0.2407$ in

Under increment in prestressing and poststressing due to truck loading equation (2.36)

$\delta^{\Delta P} = 0.0274$ in

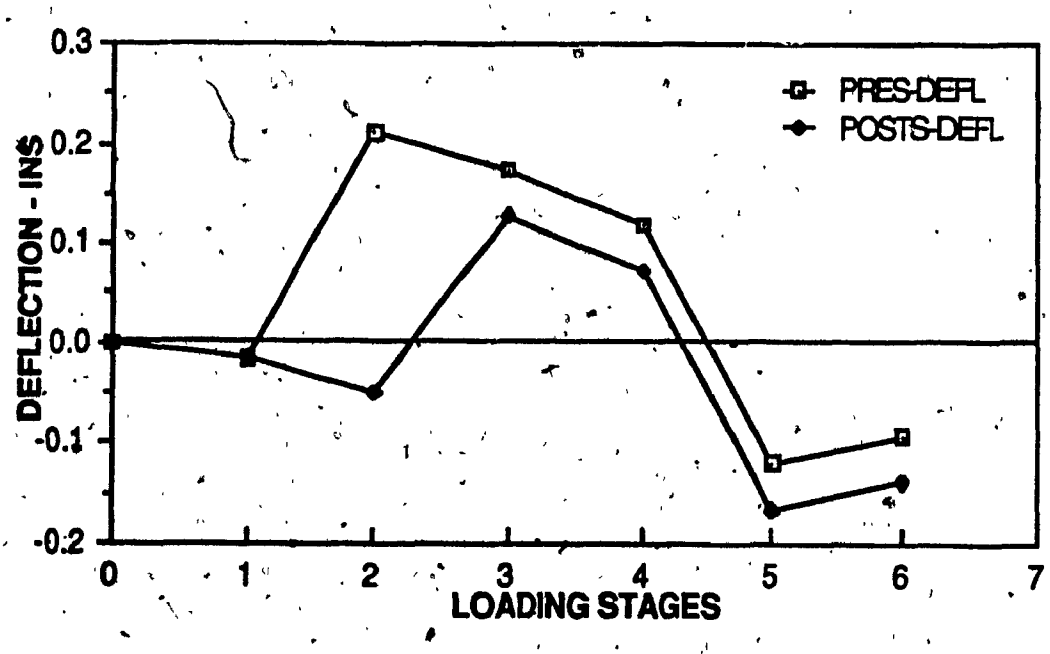

FIG A-7:- DEFLECTION OF THE GIRDER AT CRITICAL SECTION UNDER EACH STAGE OF LOADING (REF TO TABLE A-1).